Published in final edited form as:
Nature. 2016 August 25; 536(7617): 460–463. doi:10.1038/nature19074.

The TRPM2 ion channel is required for sensitivity to warmth

Chun-Hsiang Tan[1,2] and **Peter A. McNaughton**[1,*]

[1]Wolfson Centre for Age-Related Diseases, King's College London, Guy's Campus, London Bridge, London SE1 1UL, United Kingdom

[2]Department of Neurology, Kaohsiung Medical University Hospital, Kaohsiung Medical University, Kaohsiung, Taiwan

Abstract

How do we detect warmth? Thermally-activated ion channels expressed in somatosensory neurons detect the entire thermal range from extreme heat (TRPV2), painful heat (TRPV1, TRPM3, ANO1), non-painful warmth (TRPV3 and TRPV4) and non-painful coolness (TRPM8) through to painful cold (TRPA1)1–7. Genetic deletion of each of these ion channels, however, has only modest effects on thermal behaviour in mice6–12, with the exception of TRPM8, whose deletion has marked effects on the perception of moderate coolness in the range 10°C - 25°C13. The molecular mechanism responsible for detecting non-painful warmth, in particular, is unresolved. Here we used calcium imaging to identify a population of novel thermally-sensitive somatosensory neurons which do not express any of the known thermally-activated TRP channels. We then used a combination of calcium imaging, electrophysiology and RNA sequencing to show that the ion channel generating heat sensitivity in these neurons is TRPM2. Autonomic neurons, usually thought of as exclusively motor, also express TRPM2 and respond directly to heat. Mice in which TRPM2 had been genetically deleted showed a striking deficit in their sensation of non-noxious warm temperatures, consistent with the idea that TRPM2 initiates a "warm" signal which drives cool-seeking behaviour.

Previous studies have described novel heat-sensitive neurons not activated by agonists for any of the known heat-sensitive ion channels5,14–16. We identified these neurons in cultures from dorsal root ganglia (DRG) by using calcium imaging and selective agonists for known thermo-TRP ion channels. Around 10% of neurons express a novel heat-sensitive mechanism (see Fig 1A-C and Supplementary Information video 1). Changing the order of application of agonists or using a lower starting temperature had little effect on this proportion (Extended Data Figs. 1, 2). Novel heat-sensitive neurons were found to be activated over a wide range of temperatures, with a subset activated in the range of warm temperatures between 34°C and 42°C, suggesting a possible role in warmth sensation, and a second group activated only at higher temperatures (Fig. 1D, E). Novel heat-sensitive

*To whom correspondence should be addressed: peter.mcnaughton@kcl.ac.uk.

Author contributions

C.-H.T. designed and performed experiments, analysed data and wrote the paper. PMcN designed experiments, analysed data, supervised the work and wrote the paper.

Europe PMC Funders Author Manuscripts

neurons were significantly larger than either TRPV1 expressing or TRPM3-expressing neurons (Extended Data Fig. 3). We investigated the possibility that the novel heat-sensitive mechanism may be co-expressed with TRPV1 and TRPM3 by blocking these channels with antagonists before applying heat; the higher proportion of neurons responding (46% in Extended Data Fig. 4A, compared to <10% expressing only the novel heat-sensitive mechanism, see Fig. 1 and Extended Data Figs 1, 2, 4B) shows that there is significant co-expression. The phenotype of neurons expressing the novel heat-sensitive mechanism was investigated by identifying novel heat-sensitive neurons in the presence of TRP channel blockers (red in Fig 5A) and then exposing to IB4, which marks a non-peptidergic neuronal population (green in Extended Data Fig 5B). These results show that the novel heat-sensitive mechanism is predominantly expressed in $IB4^+$ neurons (74% $IB4^+$).

We next sought to identify a source of neurons which expresses a less complex set of heat-sensitive ion channels than are present in DRG neurons. In isolated sympathetic neurons from the superior cervical ganglion (SCG) we found that no neuron showed an increase in $[Ca^{2+}]_i$ to agonists of known thermo-TRP channels, but that 58% showed a significant response to heat (Fig. 2A and Extended Data Fig. 6). Similar results were obtained in parasympathetic neurons isolated from the pterygopalatine ganglion (PPG), in which 49% of neurons showed novel heat sensitivity (not shown). Autonomic neurons therefore express the novel heat-activated ion channel in isolation, which offers an advantageous preparation for determining its properties.

We found that the heat-activated calcium increase in autonomic neurons was due to an influx of Ca^{2+} from the external solution, and that it was reduced but not abolished by removal of external Na^+ (Extended Data Fig. 6C). The TRPV channel family activator 2-APB17 suppressed the heat-activated Ca^{2+} influx, and the TRPV blocker ruthenium red2 had no effect (Extended Data Fig. 6D, E), making it unlikely that the novel heat-activated mechanism is a TRPV family member. The Ca^{2+} influx was unaffected by the voltage-dependent Na channel blocker TTX at a high enough concentration to block the TTX-insensitive Na^+ channels $Na_V1.8$ and $Na_V1.9$ (Extended Data Fig. 6F). L-type Ca^{2+} channel blockers prevented firing of action potentials during simultaneous recordings of membrane voltage and intracellular calcium imaging but did not completely block the heat-activated Ca^{2+} influx (Fig. 2B; see also Extended Data Fig. 6G). These observations, taken together, show that the heat-sensitive ion channel is permeable both to Ca^{2+} and to Na^+, and that when the channel is opened by heat, the resulting depolarization activates L-type Ca channels and thus augments the calcium influx. The fact that membrane current through the novel heat-activated ion channel is carried by Na^+ and Ca^{2+} makes it unlikely that the channel is ANO1, which is permeable to chloride ions6.

We next investigated the voltage- and time-dependent behaviour of the novel heat-activated ion channel, isolated by suppressing voltage-dependent calcium, sodium and potassium currents1. The current-voltage relation was approximately linear, with a reversal potential close to zero (Fig. 2C), and the channel showed no time-dependent gating by membrane voltage (Extended Data Fig. 7). Interestingly, activation of the channel by mild warmth was strongly potentiated by hydrogen peroxide, both in autonomic neurons (Fig. 2D) and in DRG neurons (Extended Data Fig. 4C, D).

To identify the ion channel responsible for the novel heat sensitivity we carried out an analysis of mRNA expression (RNAseq). We investigated two sympathetically-derived cell lines, MAH cells18 and PC12 cells. Like primary autonomic neurons, no cell in either line responded to agonists of any of the conventional thermo-TRP channels, but a significant fraction of cells responded to heat with thermal thresholds similar to those in somatosensory neurons (Extended Data Fig. 8). We also found that the fraction of heat-sensitive neurons in both lines was reduced by differentiation to a neuronal-like phenotype (red bars, Extended Data Fig. 8).

The properties of mixed Na^+/Ca^{2+} permeability, a reversal potential near 0mV and absence of time-dependent gating by membrane potential (see above) are consistent with a member of the large TRP and CNG ion channel families. RNAseq analysis of the MAH cell line showed that detectable mRNA was present only for the seven TRP channels shown in Table 1, out of all TRP and CNG channels. TRPC3, TRPV2, TRPM4 and TRPM7 are unlikely candidates for the warmth-sensitive channel as all have non-linear IV relations19, while the warmth-sensitive ion channel is linear (see Fig. 2C). TRPC1 and TRPV2 are observed to be strongly upregulated by culture in differentiation medium (Table 1), in disagreement with the downregulation observed for the heat-sensitive ion channel (Extended Data Fig 8A). TRPV2 is activated only by extreme heat20 and TRPM4 is Ca-impermeable21, neither of which accords with the properties of the novel heat-sensitive ion channel. TRPC2 is a pseudogene in primates and seems unlikely to play an important role in behavioural warmth sensation, a fundamental property in all mammals. This leaves only TRPM2, which has a linear IV relation22, is activated at temperatures above 35°C22 and is expressed in DRG neurons23,24, as the most likely candidate for the warmth-sensitive ion channel. Thermal activation of TRPM2 is enhanced by hydrogen peroxide25 and the channel is blocked by 2-APB26, both of which are characteristics shared by the novel heat-sensitive ion channel (Fig 2D, Extended Data Figs. 4C, 4D and 6D).

We confirmed the identity of the novel heat-sensitive ion channel using calcium imaging experiments on neurons from $TRPM2^{-/-}$ mice27,28. The proportions of DRG neurons responding to TRP channel agonists were similar to those in WT neurons (Fig. 1B and Extended Data Figs 1C, 2C), but the proportion of novel heat-sensitive neurons was significantly reduced, from ~10% to around 3% (red bars in Fig. 1C; $p \leqq 0.0001$, Fisher's exact test, see also Extended Data Figs. 1, 2 and 4). Moreover, the mean amplitude of the residual heat responses in $TRPM2^{-/-}$ neurons not responding to TRP channel agonists was greatly reduced, from $F_{340/380} = 2.336 \pm 0.2060$ in WT to 0.6202 ± 0.2435 in $TRPM2^{-/-}$ (Fig. 1C; $p \leqq 0.0001$, two-tailed unpaired t test). Significantly, the sensitivity of the heat response to hydrogen peroxide was abolished by deletion of TRPM2 (Extended Data Fig 4C, D). In experiments on the thermal thresholds of novel heat-sensitive neurons (Fig. 1D, E) deletion of TRPM2 abolished almost all thermal sensitivity in the range 34°C - 42°C (reduced from 4.4% in WT to 0.9% in $TRPM2^{-/-}$, $p \leqq 0.0001$; Fisher's exact test), though some neurons still responded to temperatures in the noxious thermal range (reduced from 15% in WT to 3.1% in $TRPM2^{-/-}$, $p \leqq 0.0001$; Fisher's exact test). We also considered the possibility that TRPM2 may contribute to the heat response in DRG neurons in which it is co-expressed with TRPV1 and/or TRPM3. Deletion of TRPM2 was found not to affect the maximum amplitude of the response to heat in TRPV1-expressing neurons, but it did reduce

the response of TRPM3-expressing neurons (Extended Data Fig. 9), suggesting that co-activation of TRPM2 and TRPM3 is important in determining the heat responses of these neurons. Finally, in SCG neurons from TRPM2$^{-/-}$ mice both the numbers and response amplitudes of heat-sensitive neurons were greatly reduced (Extended Data Fig 6B).

Expression of mRNA for TRPM2 was demonstrated in heat-sensitive DRG neurons using *in situ* hybridization. TRPM2 mRNA was surprisingly abundant in neurons, being expressed in 89% of DRG neurons, but was expressed in at most a very small minority of glial cells (Extended Data Fig. 10). In prior tests for heat sensitivity in the same neurons, 42% of neurons positive for TRPM2 mRNA had responded when TRPV1 and TRPM3 were blocked. The reason why not all neurons positive for TRPM2 mRNA respond to heat is not clear, but could be due to a low conversion of mRNA into TRPM2 protein or to low trafficking to the membrane in around half of DRG neurons. However, many fewer neurons responded to heat in the population not expressing mRNA for TRPM2 (13%, see Extended Data Fig. 10), a figure that is consistent with the small number of heat-sensitive neurons still seen in DRG cultures from TRPM2$^{-/-}$ mice (see for example Fig 1B).

Finally we investigated whether genetic deletion of TRPM2 has an impact on thermal preference. The most striking behavioural difference was that WT mice avoided the non-noxious warm temperature of 38°C, while TRPM2$^{-/-}$ mice showed little preference (Fig. 3C, E and Supplementary Information video 2). The difference became much less noticeable at 43°C, where noxious heat avoidance mechanisms driven by TRPV1, TRPM3 and ANO1 come into play3–9. WT mice also showed a less strong aversion than TRPM2$^{-/-}$ mice for the non-noxious cool temperature of 23°C (Fig. 3A, E). Expression of TRPM2 therefore causes WT mice to prefer cooler temperatures over a range of temperatures extending from 23°C to above 38°C, though we note that the actual temperature at the sensory nerve ending will be higher than the plate temperature, particularly at the lower end of this range, because of the influence of body temperature.

The work presented here shows that TRPM2 accounts for a novel heat sensitive mechanism in both somatosensory and autonomic neurons. The altered thermal preference in TRPM2$^{-/-}$ mice supports the hypothesis that TRPM2 expressed in somatosensory neurons provides a non-noxious “warm” signal which drives mice to seek cooler temperatures over a wide temperature range, from 23°C to above 38°C. Other studies have shown that TRPM8 provides a “cool” signal which drives warmth-seeking behaviour over the range 10°C - 25°C13, while activation of TRPV1, TRPM3 and ANO1 provide a high-temperature noxious heat avoidance signal3–9.

Methods

Animals

All *in vitro* experiments used C57BL/6 mice younger than 5 weeks old, except for adult DRG temperature threshold experiments (e.g. Fig. 1 C, D), in which 3 month old adult mice were used (these mice were from the same group as was used for two-plate thermal preference tests experiments, see Fig. 3). TRPM2 KO mice were kind gifts from Professor Yasuo Mori, and were generated as reported previously27,28. Mice were maintained on a

12h day/12h night cycle. All mice used in two-plate thermal preference tests had been backcrossed onto the parental C57Bl6/6J strain for 7 generations, and WT and TRPM2$^{-/-}$ mice were littermates from breeding pairs of TRPM2$^{+/-}$ heterozygote mice.

Primary neuron cultures

PPG, SCG and paravertebral chain ganglia were extracted from 3 or more mice and DRG from a single mouse. Ganglia were incubated in papain (2 mg/ml in Ca^{2+} and Mg^{2+}-free HBSS) for 30 min at 30°C, followed by incubation in collagenase (2.5 mg/ml in Ca^{2+} and Mg^{2+}-free HBSS) for 30 min at 37°C. Ganglia were re-suspended and mechanically dissociated in Neurobasal-A/B27 growing medium, which was prepared with Neurobasal®-A Medium supplemented with 0.25% (v/v) L-glutamine-200 mM (Invitrogen), 2% (v/v) B-27® Supplement (Invitrogen), 1% (v/v) penicillin-streptomycin (Invitrogen), and nerve growth factor (NGF) (Sigma-Aldrich) at 50 ng/ml. Dissociated neurons were centrifuged and plated onto coverslips pre-coated with poly-L-lysine (10 μg/ml) and laminin (40 μg/ml). Neurons were kept in a 37°C incubator with a 95% air/5% CO_2 atmosphere for at least 3 h before use, and all neurons were used within 24h.

PC12 cell cultures

The growth medium used for PC12 cell culture was RPMI-1640 (Sigma-Aldrich), supplemented with: 1% (v/v) penicillin-streptomycin (Invitrogen), 1% (v/v) L-glutamine-200 mM (Invitrogen), 10% (v/v) horse serum (Invitrogen) and 5% (v/v) fetal bovine serum (FBS, Invitrogen). The differentiation medium for PC12 cells was RPMI-1640 supplemented with: 1% (v/v) penicillin-streptomycin (Invitrogen), 1% (v/v) L-glutamine-200 mM (Invitrogen), 1% (v/v) horse serum (Invitrogen), and NGF (Sigma-Aldrich) with final concentration at 100 ng/ml. PC12 cells were incubated and maintained in a 37°C incubator with a 95% air/5% CO_2 atmosphere. Medium was changed every 2 days, and cells were split every 3-4 days when grown to 90% confluency. The PC12 cells were seeded for imaging on coverslips pre-coated with poly-L-lysine (1 mg/ml; Sigma-Aldrich) and collagen IV (1 mg/ml; Sigma-Aldrich). PC12 cell lines were not authenticated.

MAH cell cultures

MAH cells were kind gifts from Aviva Tolkovsky and Susan Birren18. The growth medium used for MAH cell culture was L-15 medium (Sigma-Aldrich) supplemented with: 1% (v/v) penicillin-streptomycin (Invitrogen), 1% (v/v) L-glutamine-200 mM (Invitrogen), 10% (v/v) fetal bovine serum (FBS, Invitrogen), 17% (v/v) $NaHCO_3$ (150 mM), and dexamethasone (Sigma-Aldrich) at 5 μM. The cell line was not tested for mycoplasma contamination. The differentiation medium for MAH cells was the same as the growth medium except dexamethasone was replaced with a cocktail of neurotrophic factors: CNTF (10 ng/ml; Peprotech), bFGF (10 ng/ml; Peprotech), and NGF (50 ng/ml; Sigma-Aldrich). Medium was changed every 2 days and MAH cells were split every 4 days when grown to 90% confluency and incubated and maintained in a 37 °C incubator with a 95% air/5% CO_2 atmosphere. MAH cells used for imaging were seeded on coverslips pre-coated with poly-L-lysine (1 mg/ml; Sigma-Aldrich) and laminin (40 μg/ml; BD Science). MAH cell lines were not authenticated.

Extracellular solutions and perfusion system for electrophysiology

Unless otherwise specified, all experiments were carried out with extracellular solution containing 140 mM NaCl, 4 mM KCl, 1.8 mM $CaCl_2$, 1 mM $MgCl_2$, 10 mM HEPES and 5 mM glucose; pH was adjusted to 7.4 with NaOH and osmolarity was between 295-305 mOsm. Sodium-free extracellular solution is prepared with the formulation above except for replacing sodium chloride with equimolar choline chloride. Calcium-free extracellular solution is prepared with the formulation above except for removal of calcium chloride. An 8 line manifold gravity-driven system controlled by an automated solution changer with a common outlet was used to apply solution to the cells. The temperature in three lines was heated or cooled with a Peltier device regulated by a proportional gain feedback controller designed by Dr. V. Vellani (CV Scientific, Inc). The temperature in each experimental protocol was recorded by a miniature thermocouple immediately before the solution entered the bath or (in separate control experiments) at the cell location at the tip of the solution outlet. All compounds applied were prepared as stock solutions first and then diluted to the concentration needed before experiments. Capsaicin was dissolved in ethanol to make 5 mM stock solutions. Pregnenolone sulphate was dissolved in DMSO to make 500 mM stock solutions. 2-APB was dissolved in DMSO to make 500 mM stock solutions. The TRPV4 agonist, PF-4674114, was dissolved in DMSO to make 5 mM stock solutions. Nifedipine was dissolved in DMSO to make 100 mM stock solutions. TTX was dissolved in pH 4.8 citrate buffer to make 100 mM stock solutions. Verapamil, ruthenium red, and H_2O_2 were dissolved in extracellular solution on the day of experiments.

Calcium imaging

Cells were loaded with 5 μM fura-2, AM (Invitrogen) with 0.02% (v/v) pluronic acid (Invitrogen) in growth medium for 30 min. After loading, coverslips were put in an imaging chamber and transferred to a Nikon Eclipse Ti-E inverted microscope. Cells were continuously perfused with extracellular solution and were illuminated with a monochromator alternating between 340 and 380 nm (OptoScan; Cairn Research), controlled by WinFluor 3.2 software (Dr. John Dempster, University of Strathclyde, Glasgow, UK). Emission was collected at 510 nm and the resulting pairs of images were acquired every two seconds with a 100 ms exposure time using an iXon 897 EM-CCD camera (Andor Technology, Belfast, United Kingdom). Image time series were converted to .tiff and processed with ImageJ software. Images of the background fluorescence intensity were obtained for both wavelengths and subtracted from the respective image stack before calculating the $F_{340/380}$ ratio images. A minority of neurons (<10%) exhibited an unstable $F_{340/380}$ baseline in the absence of any applied stimulus, usually caused by poor dye loading but in some cases apparently due to low-frequency repetitive firing even in the absence of any treatment, and were removed from analysis. In experiments to identify neurons responding to known TRP channel agonists (Fig. 1A), we found that PS caused a very slow increase in $F_{340/380}$ ratio in some neurons, clearly distinguishable from the rapid elevation in $[Ca]_i$ seen in TRPM3-expressing DRG neurons. This slow response can probably be attributed to an off-target effect of PS as it was also seen in autonomic neurons which do not appear to express TRPM3 (Fig. 2). A positive response to all agonists was therefore defined from the rate of increase of $[Ca]_i$ following agonist application, as an increase of $F_{340/380}$ ratio, between two consecutive time points following application of agonist, which exceeds

the mean + 3.09 SD (cumulative probability value of 99.9%) of all such differences in the absence of any agonist. A heat-sensitive neuron is defined as a neuron with a peak increase in $F_{340/380}$ during a heat stimulus larger than the mean + 3.09 SD of the peak increase in $F_{340/380}$ of the glial cells in the same experiment (see Fig. 1B). The thermal threshold of a heat-responsive neuron (see Fig. 1D, E) was defined as the temperature when the increase in $F_{340/380}$ ratio between two consecutive time points is larger than the mean + 3.09 SD of the increase in $F_{340/380}$ of the glial cells between two consecutive time points in the same experiment. For MAH and PC12 cell cultures, where no glial cells were present, we used the value of mean + 3.09 SD obtained from glial cells in similar experiments on neuronal cultures.

Supplementary Information video 1 shows an example series of calcium images.

Patch clamp recordings

The intracellular solution for concurrent calcium imaging and patch clamp (see Fig. 2B) contained 140 mM KCl, 1.6 mM $MgCl_2$, 2.5 mM MgATP, 0.5 mM NaGTP, 2 mM EGTA, 10 mM HEPES and 167 μM fura-2; pH was adjusted to 7.3 with KOH. The intracellular solution for current-voltage relationship determination, in which Ca^{2+} and K^+ currents were blocked (see Fig. 2D), contained 130 mM CsCl, 2.5 mM MgATP, 0.5 mM NaGTP, 10 mM HEPES, 10 mM TEA, and 5 mM 4-AP; pH was adjusted to 7.3 with CsOH. The osmolarity of both of the intracellular solutions was between 295-305 mOsm. The extracellular solution for current-voltage relationship determination contained 125 mM NaCl, 2 mM $CaCl_2$, 10 mM HEPES and 5 mM glucose, 10 mM TEA, 5 mM 4-AP, 2μM tetrodotoxin, and 100 μM $CdCl_2$.

All patch clamp experiments were carried out with an Axopatch 200B patch-clamp amplifier (Axon Instrument, USA). Patch pipettes (Blaubrand 100 μl borosilicate glass, Scientific Laboratory Supplies, Germany) were pulled using a Flaming/Brown P-97 horizontal micropipette puller (Sutter Instruments, USA) and had a resistance between 3 and 5.5 MΩ. A giga-ohm seal was formed between the patch pipette and the cell membrane and the pipette capacitance transients were cancelled before achieving the whole cell configuration. All experiments were begun in voltage clamp mode with holding potential at -60 mV at the time of entering whole cell mode. After entering the whole-cell mode, series resistance was adjusted to be lower than 20 mega-ohm. Resting membrane potential was tested and only neurons with membrane potentials more negative than -50 mV were used for recording. Data were acquired and analysed with pClamp10 software (Axon Instruments, USA) and whole cell currents and voltages were filtered at 1 kHz and sampled at 10 kHz.

RNA-seq

MAH cells were trypsinized and collected as a cell pellet prior to lysis. RNA extraction was performed with the miRNeasy Mini Kit (Qiagen) according to the manufacturer's instructions. 2 samples from MAH cells grown in growth medium and 2 samples from MAH cells grown in differentiation medium were sent to Oxford Gene Technology to complete the rest of the steps for RNA-sequencing. Sequencing libraries were prepared with the Illumina TruSeq RNA Sample Prep Kit v2. A total of 4 samples (two cold-sensitive MAH cells and

two cold-insensitive MAH cells) were sequenced on 2 lanes on the Illumina HiSeq2000 platform using TruSeq v3 chemistry. All sequences were paired-end and performed over 100 cycles. Read files (Fastq) were generated from the sequencing platform via the manufacturer's proprietary software. Reads were processed through the Tuxedo suite. Reads were mapped to their location to the appropriate Illumina iGenomes build using Bowtie version 2.02. Splice junctions were identified using TopHat, version v2.0.9. Cufflinks version 2.1.1 was used to perform transcript assembly, abundance estimation and differential expression and regulation for the samples. Visualisation of differential expression results were performed with CummeRbund. RNA-Seq alignment metrics were generated with Picard.

In situ hybridization following calcium imaging

Coverslips were marked on the periphery with a diamond knife to assist localization of the imaged region and were then calcium-imaged as above to identify novel heat-sensitive neurons. Following calcium imaging, coverslips were rinsed with phosphate-buffered saline (PBS) then fixed in 4% paraformaldehyde (PFA) at 4°C for 20 min. TRPM2 mRNA was detected with Digoxigenin-labeled antisense probes against mouse TRPM2 (NM_138301.2). We are very grateful to Prof. Yasuo Mori of Kyoto University for providing the mouse TRPM2 gene cloned into the pCI-neo plasmid (Promega).

Probe synthesis—For the TRPM2 antisense probe the plasmid was linearized with EcoRI and transcribed with T3 RNA polymerase and for the TRPM2 sense probe, which was used as a negative control, the plasmid was linearized with SalI and transcribed with T7 RNA polymerase.

Hybridization—Fixed coverslips were rinsed in PBS with 0.1% Triton, and were then incubated in *in situ* hybridization solution without probe at 47°C for 30 min as pre-hybridization step. After pre-hybridization, coverslips were transferred into *in situ* hybridization solution with antisense or sense probes for hybridization at 47°C overnight29.

Post-hybridisation steps—Following hybridization coverslips were washed in 2 x SSC and then 0.2 x SSC at 47 °C for 30 min for each solution. Coverslips were then washed twice with KTBT solution at room temperature for 5 min for each washing. 25% normal goat serum was then used for blocking cells for 1 h at room temperature. Coverslips were then incubated in 25% normal goat serum containing pre-absorbed anti-digoxygenin antibody coupled to alkaline phosphatase for 2 h at room temperature, followed by washing 3x in KTBT for 15 min each wash, and then twice in alkaline phosphatase buffer at room temperature for 10 min each wash. Coverslips were then developed in alkaline phosphatase buffer containing 337.5 μg/ml NBT and 175 μg/ml BCIP in the dark for 8 h before being washed in KTBT, fixed in 4% PFA for 10 min, washed in PBS, and then mounted in 29SlowFade Gold Antifade Mountant with DAPI. DIC transmitted-light images were acquired through a Plan Fluor 10x Ph1 DLL objective with a DS-Qi2 monochrome camera on a Nikon Eclipse Ti-E inverted microscope. A GFPHQ filter was used to enhance the dark purple color. The images were rotated, cropped, and resized with ImageJ to be aligned with the images obtained in calcium imaging.

Staining for isolectin B4 (IB4) following calcium imaging

DRG neurons on marked coverslips were calcium imaged as above then rinsed with phosphate-buffered saline (PBS) and fixed in 4% paraformaldehyde (PFA) at 4°C for 20 min. After fixation, coverslips were washed twice in PBS with 0.1% Triton then incubated in solution containing 10 μg/ml IB4 bound to Alexa Fluor 594, 10% normal goat serum, 2% bovine serum albumin, 0.1% Triton, and 10 mM sodium azide for 1 h at room temperature followed by washing with PBS three times. DIC transmitted-light images were acquired through a Plan Fluor 10x Ph1 DLL objective with a DS-Qi2 monochrome camera on a Nikon Eclipse Ti-E inverted microscope. A Texas Red HYQ filter was used to capture the Alexa 594 signal. The images obtained were rotated, cropped, and resized with ImageJ to be aligned with the images obtained in calcium imaging.

Two-plate thermal preference tests

To eliminate as far as possible any extraneous genetic influences the TRPM2$^{-/-}$ mice were backcrossed onto the parental C57Bl6/6J line for 7 generations27,28. To minimize environmental effects, WT and TRPM2$^{-/-}$ littermates from heterozygous matings were compared in behavioural experiments. Sample size to achieve significance was determined from trial experiments, and all mice were tested at all temperatures (see Fig. 3 legend). We used a two-plate thermal preference test with one plate maintained at a temperature of 33°C, which other studies have shown is the preferred temperature11, and the other at a variable temperature. The temperatures of test and control plates were reversed after 30min to control for any influence of environmental cues. Other studies have observed sex differences in mouse thermal behaviour12 so we followed other authors5,11 in using only adult males (10-16 weeks old) in behavioural experiments.

Two hot/cold-plate machines (Bioseb, France), placed back to back, formed the two-plate thermal apparatus. Plates were enclosed in a plexiglass chamber divided into two lanes, with an opaque compartment between them, and two mice were tested simultaneously in adjacent lanes (see Supplementary Information video 2). The temperature of each plate was controlled by T2CT software (Bioseb, France). Plate temperatures were tested with an infrared thermometer (Bioseb) and were found to be accurately controlled to within 0.2 °C of the command temperature over the entire plate area. One plate was maintained at the preferred temperature of 33°C, and mice were initially placed onto the plate with starting temperature other than 33°C (“plate A”, see Fig. 3) before initiating recording. The movements of the mice between the two plates were recorded for 3495 seconds without human presence and the mouse position was determined with an automated video tracking system (Bioseb), so operator blinding was not necessary. The temperatures of the two plates were exchanged 1800 seconds after initiation of recording; plate temperature settled to within 0.2°C of the new temperature within 180s of the change. Experiments were performed between 8am and 10pm with room temperature at 20°C. All mice were tested at all temperatures, so randomization for the purposes for group allocation was not needed. For experiments testing thermal preference between the two mildest temperatures, 28°C vs 33°C and 33°C vs 38°C, mice were tested again, with the starting temperatures of the two plates exchanged, 3-5 h after the first recording. For other temperatures recordings were made only once on a particular mouse. Mice were tested with the protocols, in order, of 28°C vs 33°C,

33°C vs 38°C, 23°C vs 33°C and 33°C vs 43°C. Sample size was based on pilot experiments. When making statistical comparisons variances were checked to ensure that it was similar between groups being compared. All animal experiments were approved by the Animal Welfare and Ethical Review Body (AWERB), King's College London.

Supplementary Information video 2 shows an example of a thermal-choice behavioural experiment.

Statistical analysis

All data are expressed as means ± s.e.m. Analyses were performed with GraphPad Prism version 6.01 or SigmaPlot 11.0. The particular statistical test used is stated in the text or Fig legends.

Biological and technical replicates

Biological replicates are stated in the legends for each Figure. In the nature of these experiments technical replicates were not possible.

Europe PMC Funders Author Manuscripts

Extended Data

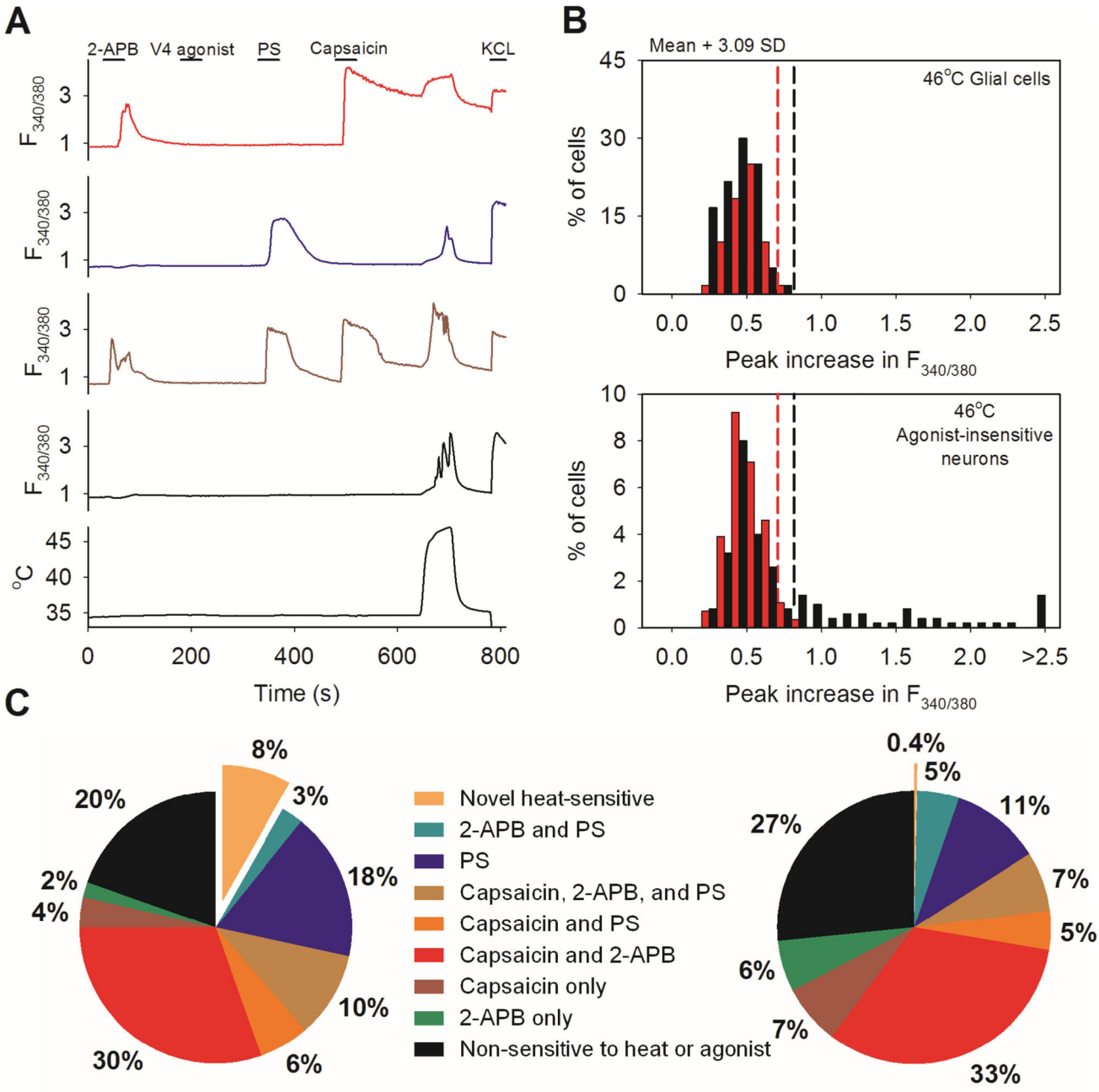

Extended Data Fig. 1. Effect of altering the order of agonist application in DRG neurons

A. Method for detecting novel heat-sensitive somatosensory neurons. Representative traces showing increases of $[Ca^{2+}]_i$ ($F_{340/380}$ ratio, ordinate) in DRG neurons in response to the TRPV1-3 agonist 2-APB (250μM), to the specificTRPV4 agonist PF-4674114 (V4 agonist, 200 nM), to the specific TRPV1 agonist capsaicin (Caps, 1μM), to the TRPM3 agonist pregnenolone sulphate (PS, 100μM), to a heat ramp from 35°C to 46°C (temperature protocol shown at bottom), and to KCl (50 mM). Other details as in Fig. 1. From top:

Europe PMC Funders Author Manuscripts

TRPV1-expressing neuron responding to 2-APB, capsaicin (1 μM) and heat (red, 30% of 500 neurons); TRPM3-expressing neuron responding to PS (blue, 100 μM) and heat (18%); TRPV1- and TRPM3- co-expressing neuron responding to 2-APB, PS, capsaicin, and heat (brown, 10%); neuron unresponsive to TRP channel agonists but showing a response to heat and therefore expressing a novel heat sensitive ion channel (black, 8% of total). No neuron responded to the specific TRPV4 agonist PF-4674114 (200nM).

B. Heat has a small effect on the fura-2 fluorescence ratio30, so we eliminated neurons in which an increase of fluorescence ratio was due simply to this physical effect by comparing the increase of fura-2 fluorescence ratio in neurons with that in glial cells in the same culture. Maximum increases in $F_{340/380}$ ratio in response to a heat ramp from 35°C to 46°C in WT glial cells (black bars, top, n=60) and in WT DRG neurons not responding to known thermo-TRP agonists (black bars, bottom, from same images as the glial cells in top panel, n=139). Vertical black dashed line in top panel shows mean + 3.09 SD (cumulative probability value of 99.9%) of the increase in the $F_{340/380}$ ratio in glial cells; this value is taken as the maximum increase in $F_{340/380}$ ratio caused by effect of heat on fura-2 and is used as the cut-off value for defining novel heat-sensitive neurons present in the same culture dish (vertical black dashed line in lower panel). Similar results from separate culture of $TRPM2^{-/-}$ glia (n = 40) and neurons (n= 76) shown in red. The proportion of novel heat-sensitive neurons was significantly reduced from 8% (41/500) in WT to 0.4% (1/282) in $TRPM2^{-/-}$ ($p \leqq 0.0001$; Fisher's exact test). The increases in $F_{340/380}$ ratio of novel heat-sensitive neurons above the cut-off value in response to heat (smallest increase = 0.019854) are all higher than that of the single heat-responding $TRPM2^{-/-}$ neuron (0.019084).

C. Pie charts showing the percentage of novel heat-sensitive neurons responding to TRP ion channel agonists and to heat in WT DRG neurons (left) and DRG neurons from $TRPM2^{-/-}$ mice (right). Deletion of TRPM2 reduces the percentage of novel heat-sensitive neurons from 8% to 0.4%.

Cell numbers: A,B,C: 500 DRG neurons from one WT mouse on 3 coverslips and 282 DRG neurons from one $TRPM2^{-/-}$ mouse on 2 coverslips were imaged. No further replicates performed.

Europe PMC Funders Author Manuscripts

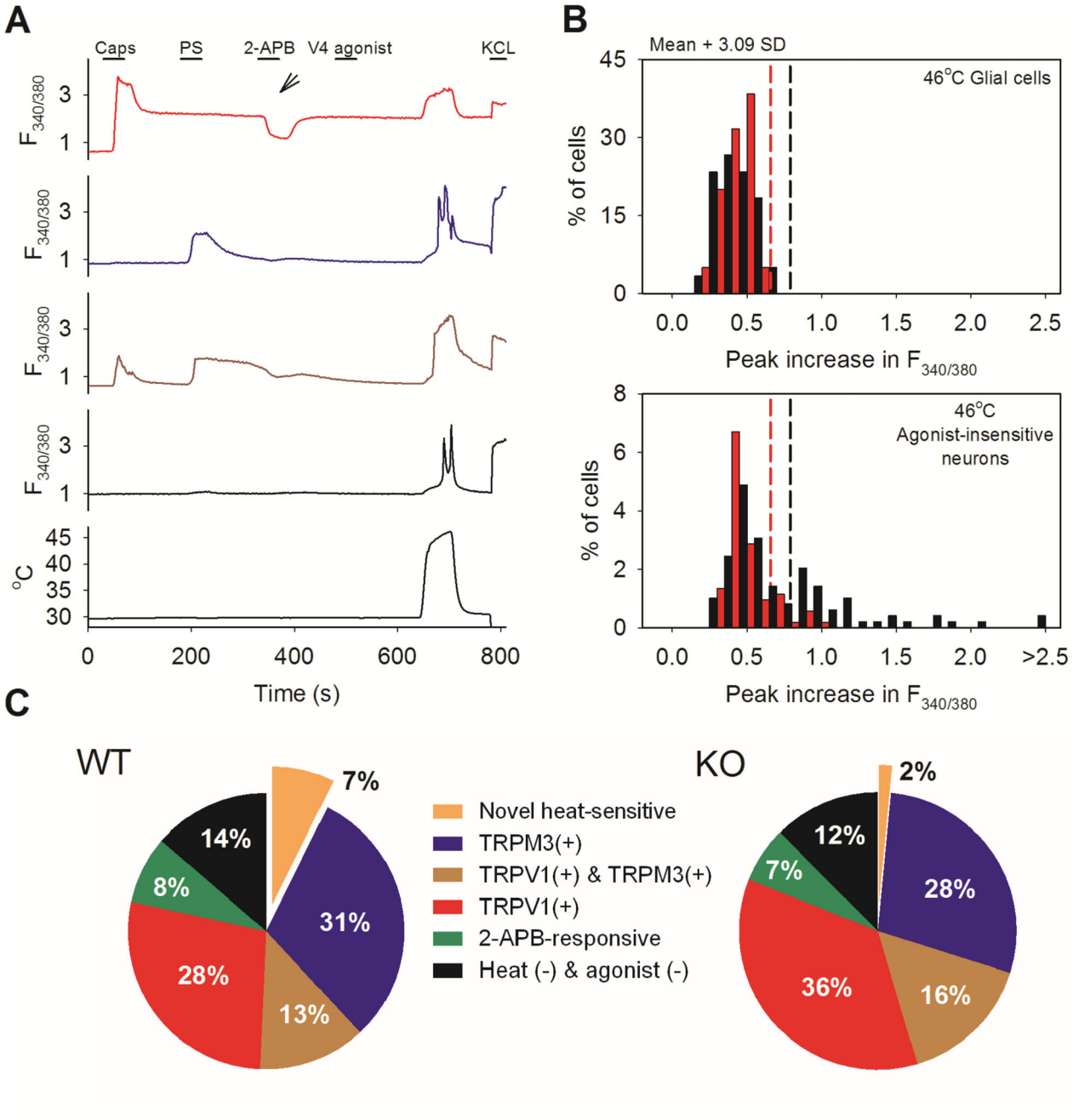

Extended Data Fig. 2. Effect of starting heat ramp at a lower temperature in DRG neurons

Identical experiment to that shown in Fig. 1A-C except that the temperature ramp started from 30°C. A. Agonist and heat-responsive neurons as in Fig. 1A. From top: TRPV1-expressing neuron responding to capsaicin (1 μM) and heat (red, 28% of 491 neurons); TRPM3-expressing neuron responding to PS (blue, 100 μM) and heat (31%); TRPV1- and TRPM3- co-expressing neuron responding to capsaicin, PS and heat (brown, 13%); neuron unresponsive to TRP channel agonists but showing a response to heat and therefore expressing a novel heat sensitive ion channel (black, 7% of total). A small number of

neurons (8%) responded to 2-APB (250μM) but not to other agonists, and 14% of DRG neurons did not respond to any of the agonists nor to heat (not shown). No neuron responded to the specific TRPV4 agonist PF-4674114 (200nM).

B. Maximum increases in $F_{340/380}$ ratio in response to a heat ramp from 30°C to 46°C in WT glial cells (black bars, top, n=60) and in heat-sensitive WT DRG neurons not responding to known thermo-TRP agonists (black bars, bottom, from same images as the glial cells in top panel, n=103). Vertical black dashed line in top panel shows mean + 3.09 SD (cumulative probability value of 99.9%) of the increase in the $F_{340/380}$ ratio in glial cells; this value is taken as the maximum increase in $F_{340/380}$ ratio caused by effect of heat on fura-2 and is used as the cut-off value for defining novel heat-sensitive neurons present in the same culture dish (vertical black dashed line in lower panel). Similar results from separate culture of TRPM2$^{-/-}$ glia (n = 60) and neurons (n= 73) shown in red. The proportion of novel heat-sensitive neurons was significantly reduced from 7% (103/491) in WT to 2% (73/522) in TRPM2$^{-/-}$ ($p \leqq 0.0001$; Fisher's exact test). The mean increase in $F_{340/380}$ ratio of novel heat-sensitive neurons above the cut-off values in response to heat was also significantly reduced from 1.237 ± 0.09207 in WT (n=36) to 0.7959 ± 0.03767 in TRPM2$^{-/-}$ (n=8) (p=0.0313; two-tailed unpaired t test).

C. Pie charts showing the percentage of novel heat-sensitive and TRPV1- or TRPM3-expressing neurons in WT DRG neurons (left) and DRG neurons from TRPM2$^{-/-}$ mice (right).

Cell numbers. A,B,C: 491 DRG neurons from one WT mouse on 3 coverslips and 522 DRG neurons from one TRPM2$^{-/-}$ mouse on 3 coverslips were imaged. No further replicates performed.

Europe PMC Funders Author Manuscripts

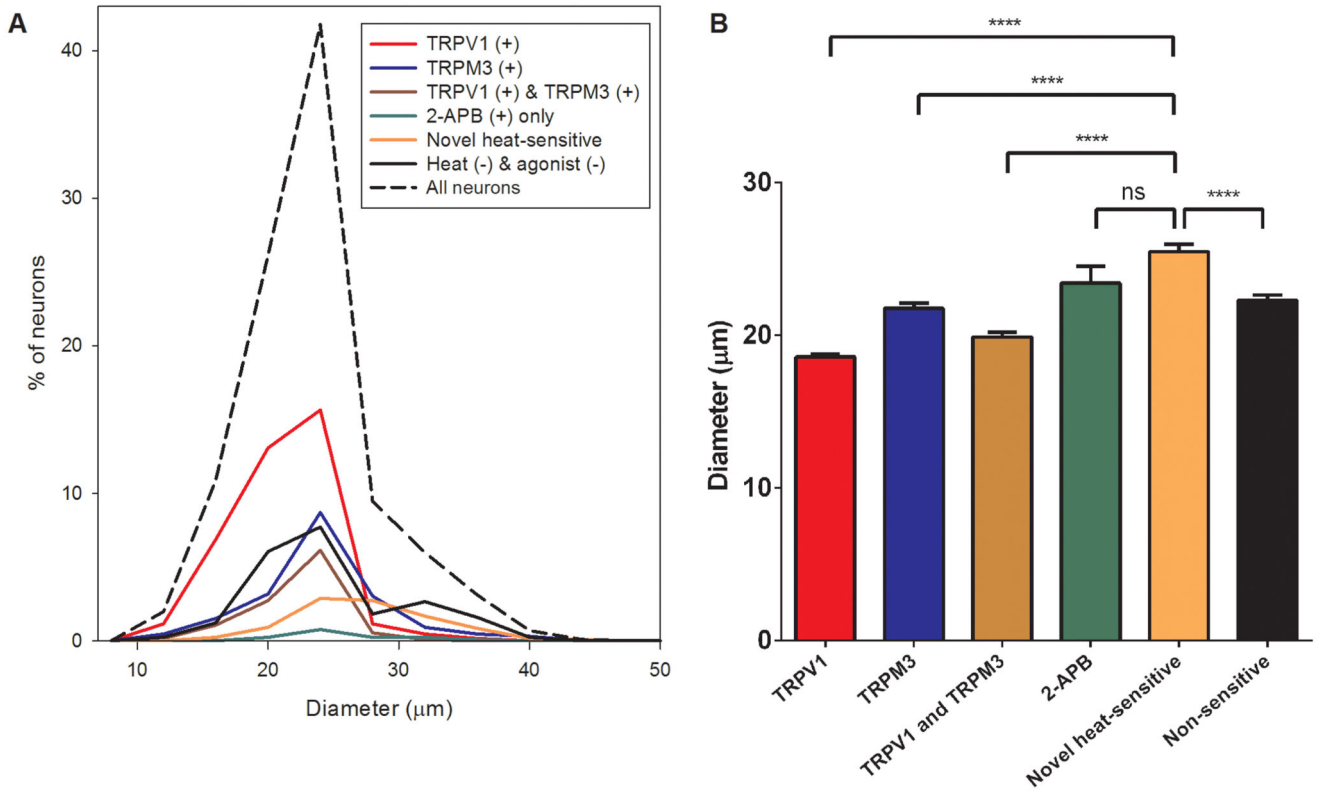

Extended Data Fig. 3. Diameters of novel heat-sensitive DRG neurons compared to neurons responding to other TRP agonists.

A. Diameters of 1324 DRG neurons taken from experiment illustrated in figure 1A (dotted line). Subpopulations of neurons are shown as follows: those responding to capsaicin and thus expressing TRPV1 (red); to PS and thus expressing TRPM3 (blue); to both agonists and thus co-expressing TRPV1 and TRPM3 (brown); to 2-APB alone (green); novel heat-sensitive neurons (orange), and neurons responding neither to heat nor to any of these agonists (black).

B. Diameter comparison of subpopulations of neurons. TRPV1-expressing neurons have the smallest mean diameter (18.58 ± 0.17μm), TRPM3-expressing neurons are intermediate (21.75 ± 0.33μm) and neurons expressing only the novel heat-sensitivity have the largest mean diameter (25.47 ± 0.48μm). Significance from one-way ANOVA and multiple comparisons with Tukey's multiple comparison test (****: ≦0.0001; ns: not significant). Cell numbers. Data obtained from Fig. 1 A, B, C; 1324 DRG neurons from one WT mouse on 4 coverslips were analysed.

Europe PMC Funders Author Manuscripts

Europe PMC Funders Author Manuscripts

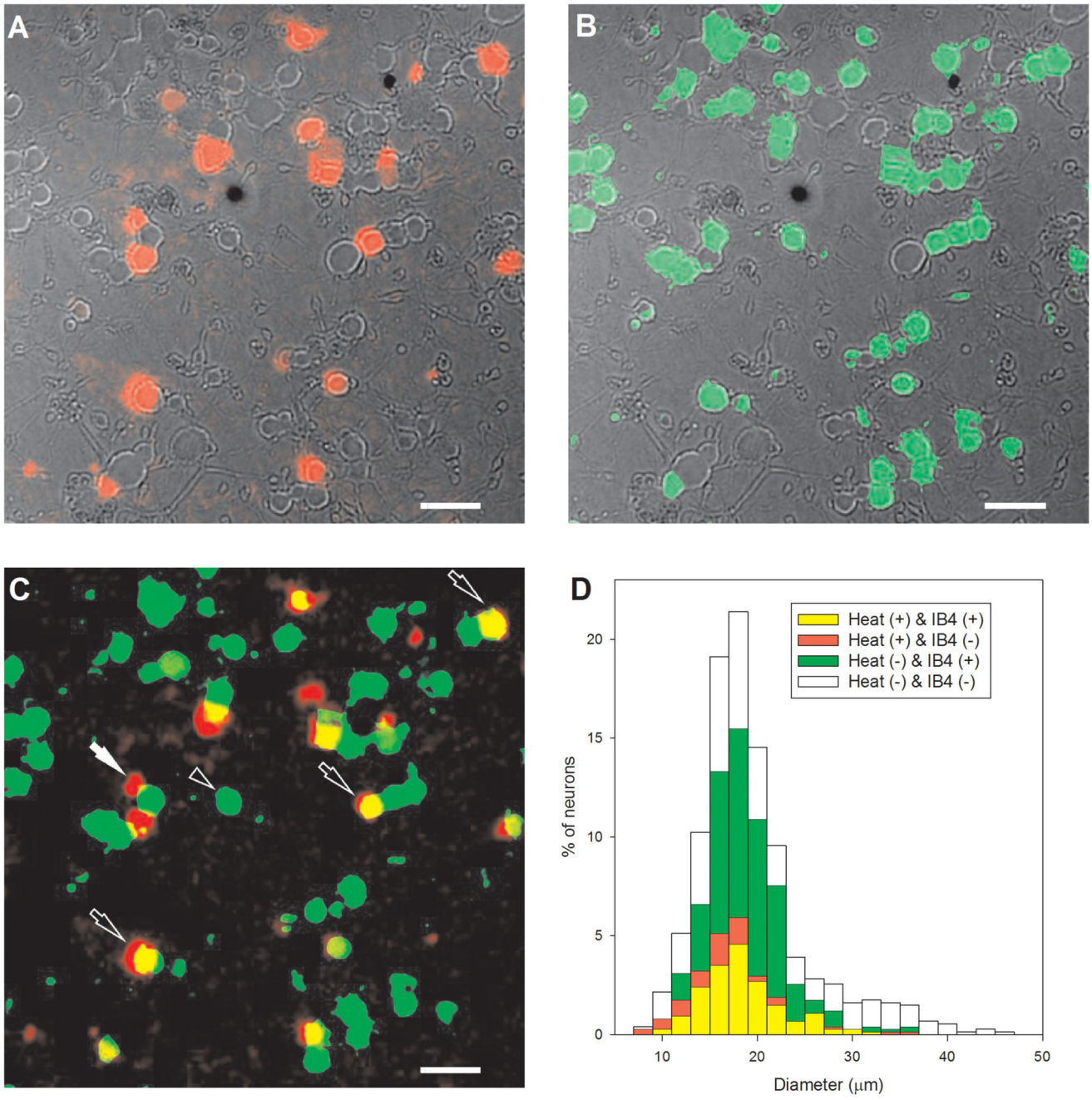

Extended Data Fig. 4. The novel heat-sensitivity in DRG neurons is partially co-expressed with TRPV1 and TRPM3, and is enhanced by H_2O_2.

A. Temperature ramp to 47°C, as in Fig. 1A, but with TRPV1 blocked with AMG9810 (5μM) and TRPM3 blocked with naringenin (10μM). Criterion level for significant increase (dashed lines) taken from glial cells in same field of view (data not shown). Black bars: 46% of all WT DRG neurons (n = 580) responded to heat ramp from 34°C to 46°C with an increase in $[Ca^{2+}]_i$ above criterion level in presence of blockers of TRPV1 and TRPM3 (dashed vertical line), while the percentage decreased to 17% in TRPM2$^{-/-}$ DRG neurons (red bars, n=1007) ($p \leqq 0.0001$; Fisher's exact test). The mean increase in $F_{340/380}$ ratio above

the cut-off values (dashed lines) in response to heat was also significantly reduced from 1.619 ± 0.06133 in WT (n=265) to 1.027 ± 0.08394 in TRPM2$^{-/-}$ (n=175) ($p \leqq 0.0001$; two-tailed unpaired t test). In similar experiments with TRPV1 blocker BCTC (4μM) and naringenin (10μM), 37% of WT neurons responded to heat (data not shown, n = 554).

B. Similar plot as in A, but data from the subgroup of novel heat-sensitive neurons not responding to agonists for known thermo-TRP channels. After exposure to heat in presence of blockers of TRPV1 and TRPM3, blockers were removed and neurons not responding to known TRP agonists were identified as in Fig. 1A. Data from same experiment as shown in A. Proportion of neurons expressing the novel heat-sensitive mechanism in isolation (i.e. without co-expression of TRPV1 or TRPM3) was significantly lower (52/580, 9%) than all neurons expressing the novel heat sensitive mechanism (46%, see A). The proportion of novel heat-sensitive neurons was significantly reduced in TRPM2$^{-/-}$ mice, from 9% to 0.6% (6/1007, $p \leqq 0.0001$; Fisher's exact test).

C. Temperature ramp to 42°C. Few novel heat-sensitive neurons respond to this low temperature in either WT or TRPM2$^{-/-}$. Total numbers of neurons n=173 for WT, n=211 for TRPM2$^{-/-}$.

D. Responses of same neurons to same temperature ramp to 42°C following addition of H_2O_2 (400μM). Enhancement of response in WT (black bars) largely abolished in TRPM2$^{-/-}$ (red bars). The proportion of novel heat-sensitive neurons after sensitization with H_2O_2 was significantly reduced from 11% (74/635) in WT to 8% (48/601) in TRPM2$^{-/-}$ (p=0.0356; Fisher's exact test). The mean increase in $F_{340/380}$ ratio of novel heat-sensitive neurons above the cut-off values in response to heat was also significantly reduced from 1.175 ± 0.1516 in WT (n=72) to 0.4485 ± 0.04329 in TRPM2-/- (n=48) (p=0.0002; two-tailed unpaired t test).

Cell numbers and replicates. A, B: 580 DRG neurons from one WT mouse on 5 coverslips and 1007 DRG neurons from one TRPM2$^{-/-}$ mouse on 5 coverslips were imaged for the protocol with AMG9810. 554 neurons from one WT mouse on 4 coverslips were imaged for the protocol with BCTC. No further replicates.

C, D: 635 DRG neurons from one WT mouse on 3 coverslips and 601 DRG neurons from one KO mouse on 3 coverslips were imaged. Experiment was replicated with similar results on 4 further coverslips from 1 mouse.

Europe PMC Funders Author Manuscripts

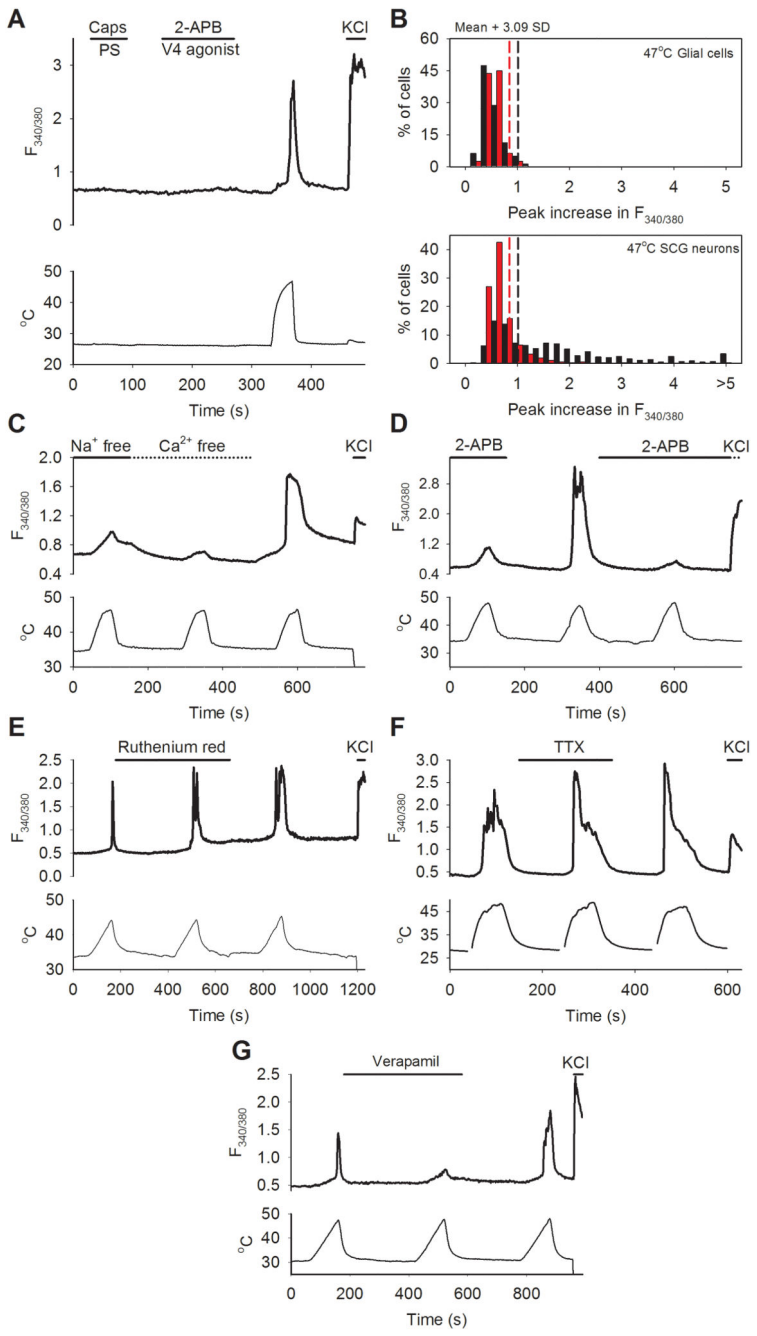

Extended Data Fig. 5. Most novel heat-sensitive DRG neurons are IB4-positive

A. Increases in $[Ca^{2+}]_i$ ($F_{340/380}$ ratio image, intensity-coded in red, mouse DRG neurons) in response to heat ramp to 46°C (TRPV1 blocked with AMG9810, 5μM, and TRPM3 blocked with naringenin, 10μM), superimposed on DIC transmission image obtained post-fixation. B. Same field following fixation and labelling with fluorescent IB4 (green). C. Superimposed calcium and IB4 images from A and B. Black arrows show neurons responding to heat and positive for IB4. White arrow shows a neuron responding to heat and negative for IB4. Black arrowhead shows neuron insensitive to heat and positive for IB4.

Scale bars 50 μm. D. Diameter histogram of 743 fixed DRG neurons subgrouped according to novel heat-sensitivity (yellow, red) and IB4 binding (yellow, green). 25% (184/743) of DRG neurons showed novel heat-sensitivity and 74% of these novel heat-sensitive neurons were IB4-positive, while only 53% of heat-insensitive neurons were IB4-positive. The percentage of IB4-positive neurons is significantly higher in the heat-sensitive group than in the heat-insensitive group ($p \leqq 0.0001$; Fisher's exact test). Note that the diameters shown in D are not directly comparable with the live cell diameters shown in Extended Data Fig 3 because of a shrinkage artifact on fixation.

Cell numbers. 743 DRG neurons from one WT mouse on 4 coverslips were imaged. No further replicates were performed.

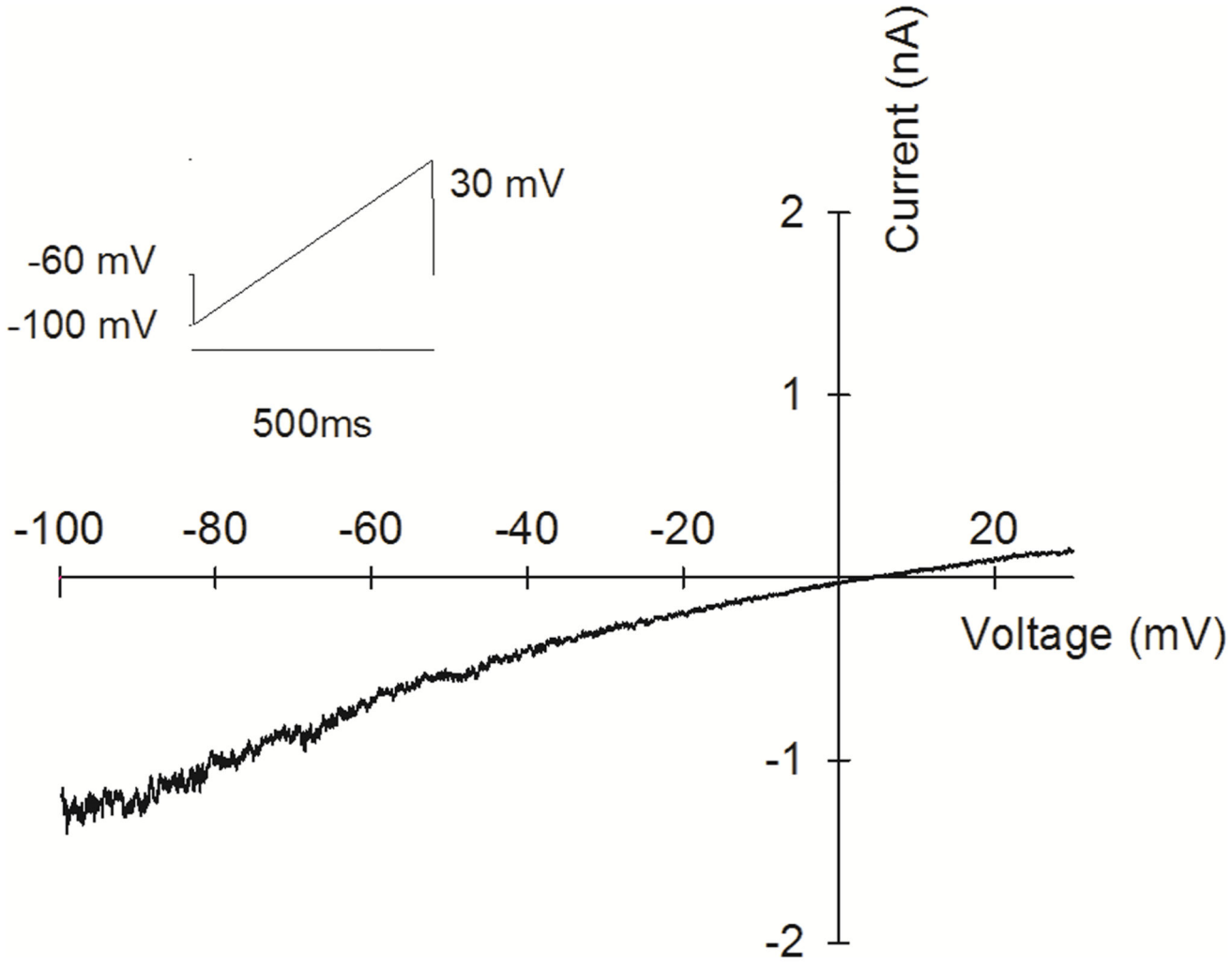

Extended Data Fig. 6. Properties of novel heat-sensitive ion channel expressed in autonomic neurons.

A. Representative traces showing increases of $[Ca^{2+}]_i$ ($F_{340/380}$ ratio, ordinate) in sympathetic neurons from superior cervical ganglion (SCG) in response to a mixture of capsaicin (TRPV1 agonist,1μM) and pregnenolone sulphate (TRPM3 agonist, 100μM); a

mixture of 2-APB (TRPV1-3 agonist, 250μM) and PF-4674114 (TRPV4 agonist, 200 nM); heat to 47°C (temperature protocol shown at bottom); and KCl (50 mM). Similar results obtained with parasympathetic neurons from pterygopalatine ganglion (PPG, data not shown). Trace is same as shown in Fig. 2A.

B. Similar histograms as in Extended Data Figs. 1B and 2B, but for SCG glial cells and neurons from WT mice (black bars) and TRPM2$^{-/-}$ mice (red bars). 58% of WT SCG neurons (n=436) showed novel heat-sensitivity with increases in $F_{340/380}$ ratio above the criterion level obtained from glial cells (n=80) in same culture (black vertical dashed line). In similar experiments on PPG neurons (n=484), 47% showed novel heat-sensitivity (not shown). Red bars and red dashed line show results from SCG glia (n=80) and neurons (n=430) from TRPM2$^{-/-}$ mice. The proportion of novel heat-sensitive neurons was significantly reduced by deletion of TRPM2, from 58% (252/436) in WT to 12% (53/430) in TRPM2$^{-/-}$ ($p \leqq 0.0001$; Fisher's exact test). The mean increase in $F_{340/380}$ ratio of heat-sensitive neurons above the cut-off values in response to heat was also significantly reduced, from 1.629 ± 0.1928 in WT (n=252) to 0.5050 ± 0.1270 in TRPM2$^{-/-}$ (n=53) (p=0.0086; two-tailed unpaired t test).

C. Heat-evoked Ca^{2+} increase in SCG neurons is reduced but not abolished by removal of extracellular Na^{+} (replaced with choline) and is abolished by removal of extracellular Ca^{2+} (remaining small increase in $F_{340/380}$ ratio is due to temperature sensitivity of fura-2, see part B). Similar results seen in 133 SCG neurons.

D. Heat-evoked Ca^{2+} increase in SCG neurons is blocked by TRPV agonist 2-APB (25μM). Similar results seen in 130SCG neurons.

E. Ca^{2+} increase in PPG neurons is not affected by TRPV channel blocker ruthenium red (50μM). Similar results seen in 75 PPG neurons.

F. Ca^{2+} increase in PPG neurons is not affected by the Na channel blocker TTX (2μM). Similar results seen in 35 PPG neurons.

G. The Ca^{2+} influx in PPG neurons is reduced but not eliminated by the L-type Ca^{2+} channel blocker verapamil (100μM). Similar results seen in 30 PPG neurons.

Cell numbers and replicates. A: 166 SCG neurons from three WT mice on 3 coverslips were imaged. B: 436 SCG neurons from two WT mice on 4 coverslips and 430 SCG neurons from two TRPM2$^{-/-}$ mice on 4 coverslips were imaged. Similar results as those shown for WT obtained with 15 further coverslips of SCG neurons from 9 WT mice and 7 coverslips of PPG neurons from 6 WT mice. C: 133 SCG neurons from 3 WT mice on 5 coverslips showed similar responses. D: 130 SCG neurons from 3 WT mice on 2 coverslips showed similar responses. Similar results also obtained for DRG neurons (4 coverslips from 1 mouse). E: 75 PPG neurons from 3 WT mice on 4 coverslips showed similar responses. F: 35 PPG neurons from 3 WT mice on 4 coverslips showed similar responses. G: 30 PPG neurons from 3 WT mice on 2 coverslips showed similar responses.

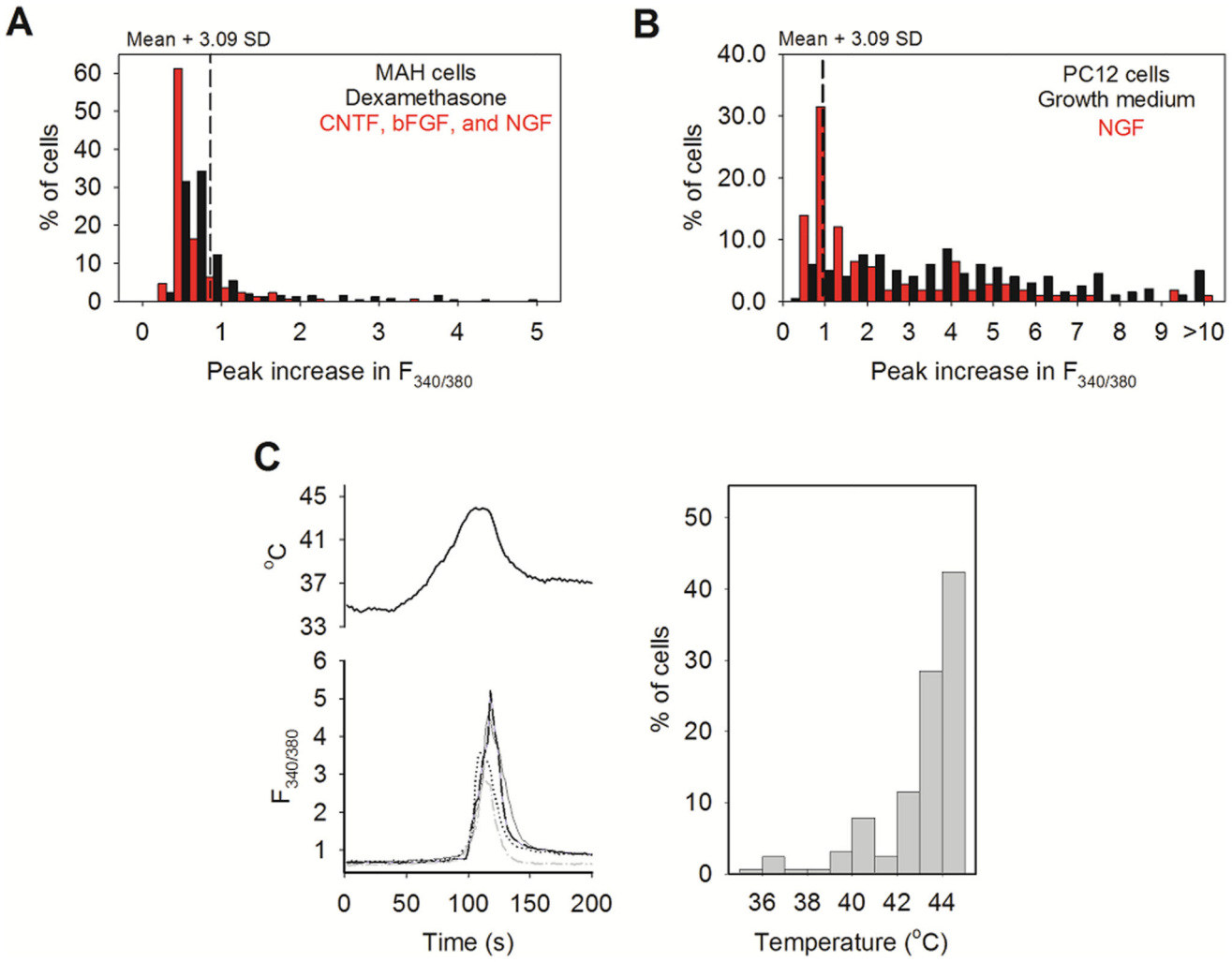

Extended Data Fig. 7. The heat-induced membrane current in autonomic neurons is not gated by membrane voltage.

Current–voltage difference relations of a PPG neuron with a voltage ramp starting from a negative potential (inset) show a similar linear heat-induced current to that obtained with reverse voltage ramp (see Fig. 2C). Trace obtained by subtracting current-voltage relations at 36°C from that at 47°C. Similar results obtained in 3 cells on 3 coverslips.

Europe PMC Funders Author Manuscripts

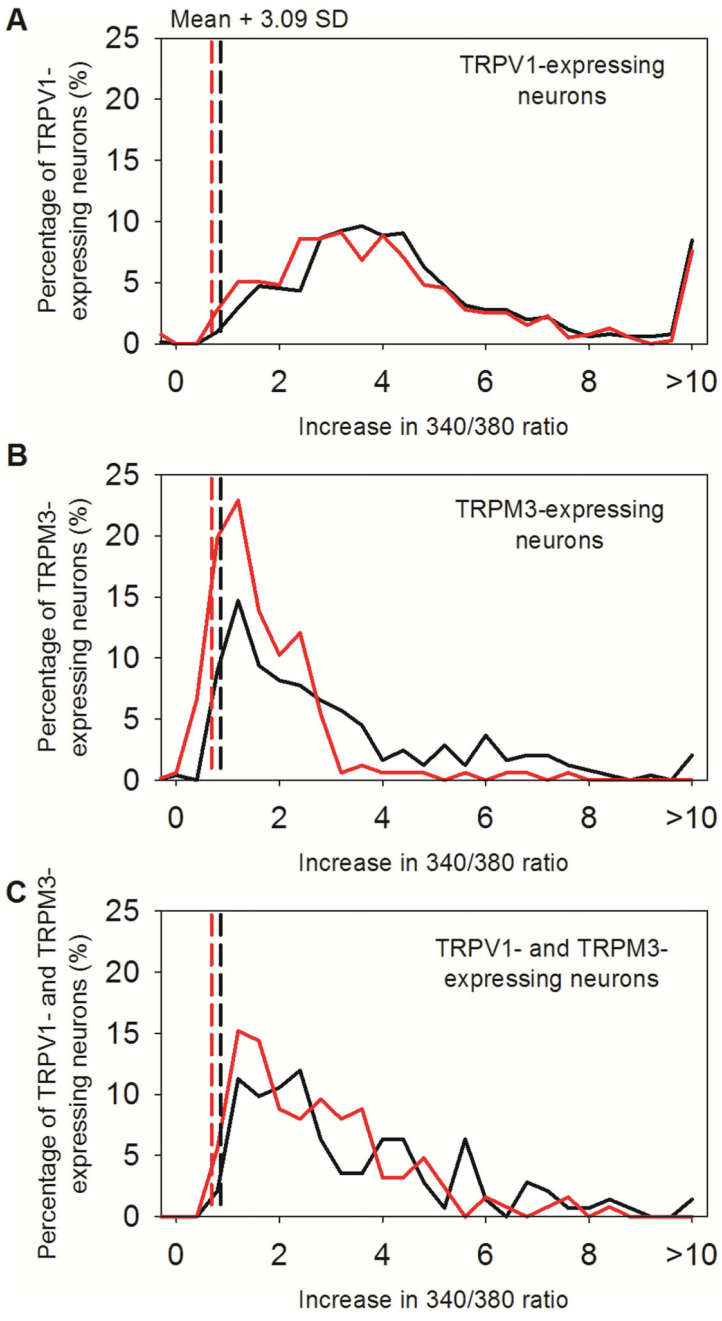

Extended Data Fig. 8. Responses to heat in adrenal-derived MAH and PC12 cell lines, and effects of factors causing differentiation to neuronal phenotype.

A. MAH cells. Black: maximum increase in $F_{340/380}$ ratio in response to heat (47°C, n = 254) when cultured in dexamethasone (5 μM). No cell responded to TRP agonists, but 27% of cells responded to heat with increase above mean criterion level obtained from glial cells in neuronal cultures (see Fig. 1B). Red: similar histogram after 12d culture in growth factors (bFGF, CNTF and NGF, see Methods, n = 170). No cell responded to TRP agonists; 9% responded to heat. The proportion of heat-sensitive cells was significantly reduced from 27% (69/254) in dexamethasone to 9% (16/170) in growth factors ($p \leqq 0.0001$; Fisher's exact test).

Europe PMC Funders Author Manuscripts

The 66% reduction in the proportion of heat-sensitive cells was not significantly different from the reduction in TRPM2 expression caused by differentiation of MAH cells (Table 1 line 5; p = 0.056; two-tailed unpaired t test). The mean increases in $F_{340/380}$ ratio above the cut-off values (dashed lines) in response to heat were 1.755 ± 0.1255 in dexamethasone (n=69) and 1.420 ± 0.1474 in presence of growth factors (n=16) (p=0.2203; two-tailed unpaired t test).

B. PC12 cells. Black: culture in growth medium (10% horse serum + 5% fetal bovine serum, n=200). 93% of cells responded to heat with increase above mean criterion level obtained from glial cells in neuronal cultures (see Fig. 1B). Red: Effect on heat responses of 12d culture in NGF (1% horse serum plus 100 ng/ml NGF, n = 108). The proportion of heat-sensitive cells was significantly reduced from 93% (186/200) in growth medium to 46% (50/108) in NGF (p≦0.0001; Fisher's exact test). We note that a significantly lower expression of mRNA for TRPM2 in differentiated PC12 cells has been reported31. The mean increase in $F_{340/380}$ ratio above the cut-off values (dashed lines) in response to heat was significantly reduced from 3.753 ± 0.2431 in growth medium (n=186) to 2.603 ± 0.3104 in NGF (n=50) (p=0.0213; two-tailed unpaired t test).

C. Temperature thresholds of PC12 cells cultured in growth medium. Top left: temperature protocol. Bottom left: temperature responses of three representative cells. Right: Temperature thresholds calculated as in Fig. 1D.

Cell numbers and replicates. A, B: 2 coverslips for each condition were imaged. Cell numbers are given above. Replicates of 4 coverslips (MAH cells) and 3 coverslips (PC12 cells) for each condition gave similar results. C: 165 PC12 cells on one coverslip were imaged.

Europe PMC Funders Author Manuscripts

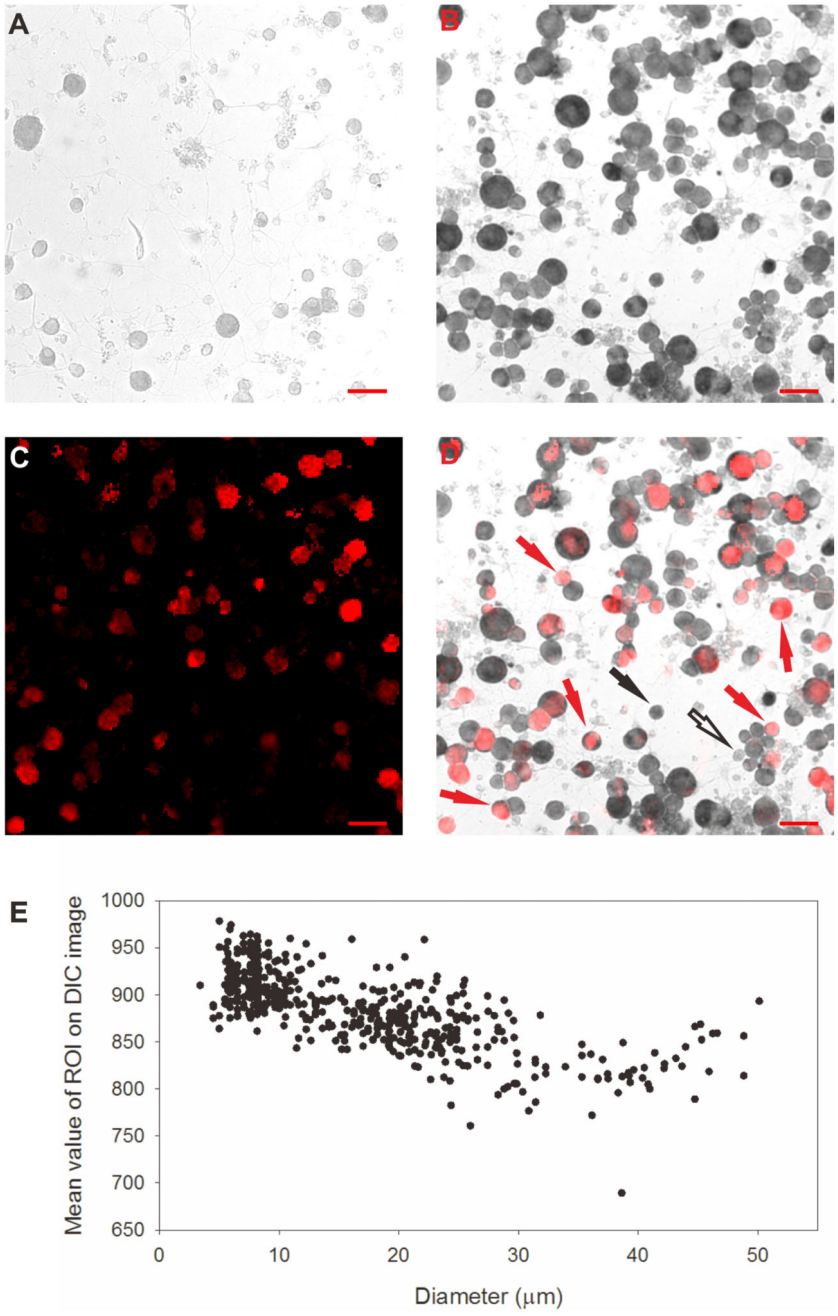

Extended Data Fig. 9. Effect of deletion of TRPM2 on maximal calcium responses to heat in neurons expressing TRPV1 or TRPM3

A. Maximum increases in $F_{340/380}$ ratio in response to a heat ramp from 34°C to 46°C in neurons responding only to capsaicin (TRPV1-expressing) from WT (black) and TRPM2$^{-/-}$ (red) mice. The increase in $F_{340/380}$ ratio in response to heat (above the increase caused by the effect of temperature on fura-2, vertical dotted lines, for method of calculation see Fig. 1B) is not significantly different between WT and TRPM2$^{-/-}$ ($p=0.1168$, two-tailed Mann–Whitney U test). Details as in Fig. 1.

B. Neurons responding only to pregnenolone sulphate (PS, TRPM3-expressing) from same experiments as in A. The increases in $F_{340/380}$ ratio in response to heat are significantly reduced by deletion of TRPM2 (from 6.389 ± 1.225 to 4.411 ± 1.582, $p<0.0001$, two-tailed Mann–Whitney U test).

C. Neurons responding to both capsaicin and PS (TRPV1- and TRPM3-expressing). The increases in $F_{340/380}$ ratio in response to heat are not significantly different between WT and TRPM2$^{-/-}$ ($p=0.0633$; two-tailed Mann–Whitney U test).

Cell numbers and replicates. A,B,C: 1324 DRG neurons from one WT mouse on 4 coverslips and 981 DRG from one TRPM2$^{-/-}$ mouse on 4 coverslips were imaged. Similar results obtained from 42 further coverslips from 6 WT mice and 8 further coverslips from 1 TRPM2$^{-/-}$ mouse.

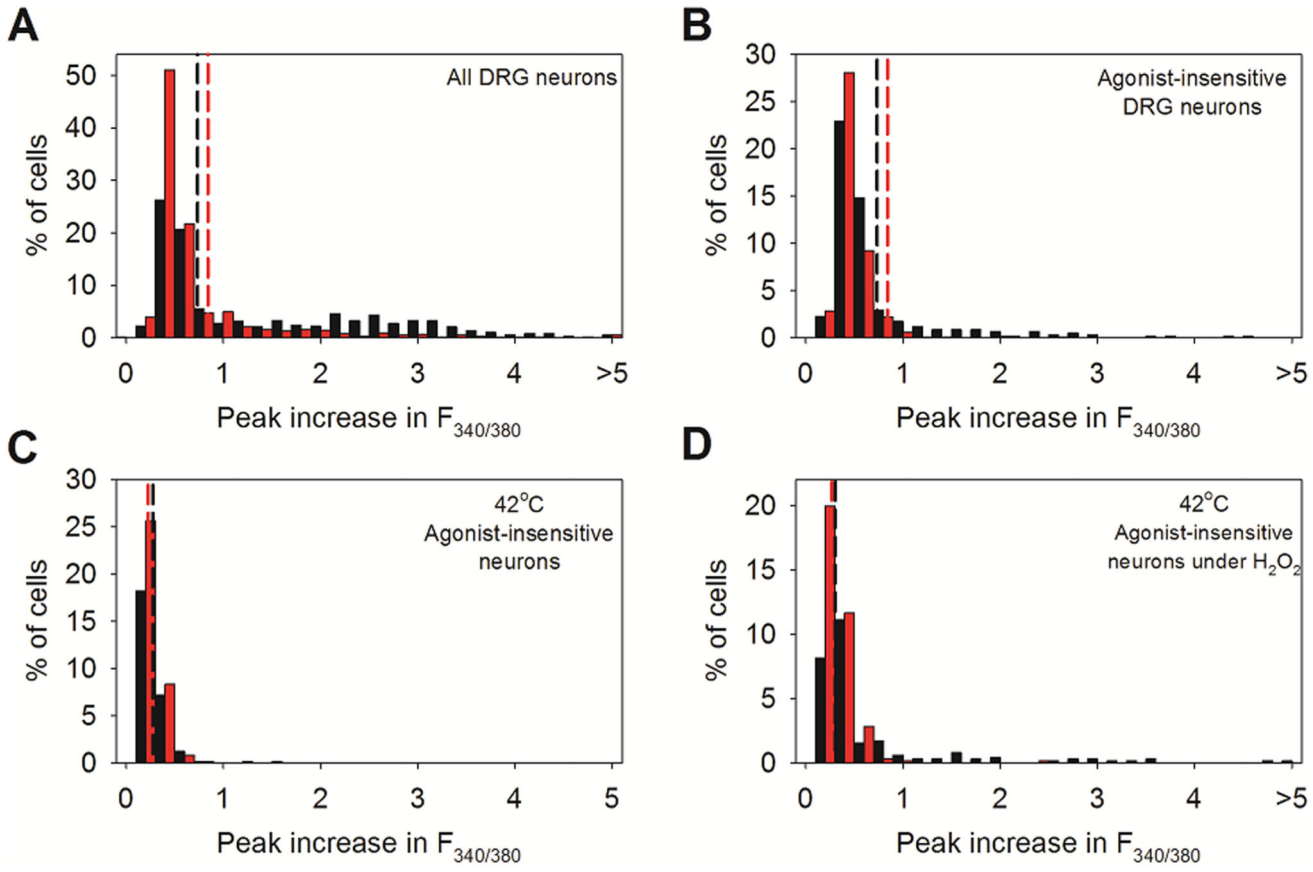

Extended Data Fig. 10. Correlation between novel heat sensitivity and expression of mRNA for TRPM2.

A. Representative DIC transmission image of DRG neurons following *in situ* hybridization with sense probe, as negative control. Non-specific density was linearly dependent on cell diameter (see E). Mean + 3.09 SD (cumulative probability value of 99.9%) of density as a function of diameter with sense probe (5μm bins) was used as threshold criterion for significant expression of TRPM2 in images of antisense hybridization. A similar analysis of non-specific density was carried out for glial cells.

B. Representative DIC transmission image with antisense probe against TRPM2. Using the threshold criterion as function of diameter obtained from sense probe images (see A), 89% (1121/1250) of DRG neurons but 3% (4/120) of glial cells were positive for TRPM2 mRNA.
C. Novel heat-sensitive DRG neurons determined using calcium imaging. Increases in $[Ca^{2+}]_i$ ($F_{340/380}$ ratio image, intensity-coded in red) in response to a heat ramp to 46°C with TRPV1 blocked with AMG9810 (5μM) and TRPM3 blocked with naringenin (10μM).
D. Superimposed image of novel heat-sensitive neurons (red) and *in situ* hybridization using antisense probe. Solid red arrows indicate novel heat-sensitive neurons also positive for TRPM2; solid black arrow shows neuron not responding to heat but positive for TRPM2; open black arrow shows cell negative for TRPM2 (i.e. with density below the criterion level obtained from E). 42% (92/218) of DRG neurons positive for TRPM2 exhibited novel heat-sensitivity. However only 13% (2/16) of DRG neurons negative for TRPM2 from in situ hybridization exhibited novel heat-sensitivity. The percentage of novel heat-sensitive DRG neurons is significantly reduced in TRPM2 negative DRG neurons (p=0.0188; Fisher's exact test). Scale bars shown on right lower corner indicate 50 μm.
E. Density of non-specific label in neurons obtained from hybridization with sense probe (see A) depends on cell size. Data used to calculate significance thresholds for neurons in B. Cell numbers and replicates. A: One coverslip exposed to sense probe was used as negative control. B: All neurons on 5 coverslips were measured and one coverslip was measured for TRPM2-positive glial cells; C, D: One coverslip was analysed as in A and B for the combined calcium imaging and *in situ* hybridization protocol. E: 500 DRG neurons on one coverslip exposed to sense probe was used to determine the background threshold as a function of cell diameter. Similar in situ hybridization results obtained on 16 further coverslips.

Supplementary Material

Refer to Web version on PubMed Central for supplementary material.

Acknowledgements

We thank Aviva Tolkovsky for help and advice, Rwei-Ling Yu for assistance with experiments, Yasuo Mori for $TRPM2^{-/-}$ mice and for the cDNA for mouse TRPM2, Susan Birren for MAH cells, John Wood for loan of the thermal preference test apparatus, Sarah Skerratt for PF-4674114, and Ewan Smith, Joan Btesh, David Andersson, and Tamara Buijs for their comments on the manuscript. Initial experiments were performed in the Department of Pharmacology, University of Cambridge. Supported by a grant from the BBSRC (UK) to PMcN and a Raymond & Beverley Sackler studentship to C-HT.

References

1. Cesare P, McNaughton PA. A novel heat-activated current in nociceptive neurons, and its sensitization by bradykinin. Proc Natl Acad Sci USA. 1996; 93:15435–15439. [PubMed: 8986829]
2. Caterina MJ, et al. The capsaicin receptor: a heat-activated ion channel in the pain pathway. Nature. 1997; 389:816–824. [PubMed: 9349813]
3. Jordt SE, McKemy DD, Julius D. Lessons from peppers and peppermint: the molecular logic of thermosensation. Curr Opin Neurobiol. 2003; 13:487–492. [PubMed: 12965298]
4. Basbaum AI, Bautista DM, Scherrer G, Julius D. Cellular and molecular mechanisms of pain. Cell. 2009; 139:267–284. [PubMed: 19837031]
5. Vriens J, et al. TRPM3 is a nociceptor channel involved in the detection of noxious heat. Neuron. 2011; 70:482–494. DOI: 10.1016/j.neuron.2011.02.051 [PubMed: 21555074]

6. Cho H, et al. The calcium-activated chloride channel anoctamin 1 acts as a heat sensor in nociceptive neurons. Nat Neurosci. 2012; 15:1015–1021. doi:nn.3111 [pii]. DOI: 10.1038/nn.3111 [PubMed: 22634729]
7. Vriens J, Nilius B, Voets T. Peripheral thermosensation in mammals. Nature reviews. Neuroscience. 2014; 15:573–589. DOI: 10.1038/nrn3784 [PubMed: 25053448]
8. Caterina MJ, et al. Impaired nociception and pain sensation in mice lacking the capsaicin receptor. Science. 2000; 288:306–313. [PubMed: 10764638]
9. Davis JB, et al. Vanilloid receptor-1 is essential for inflammatory thermal hyperalgesia. Nature. 2000; 405:183–187. [PubMed: 10821274]
10. Moqrich A, et al. Impaired thermosensation in mice lacking TRPV3, a heat and camphor sensor in the skin. Science. 2005; 307:1468–1472. [PubMed: 15746429]
11. Huang SM, Li X, Yu Y, Wang J, Caterina MJ. TRPV3 and TRPV4 ion channels are not major contributors to mouse heat sensation. Mol Pain. 2011; 7:37. doi:1744-8069-7-37 [pii]. doi: 10.1186/1744-8069-7-37 [PubMed: 21586160]
12. Miyamoto T, Petrus MJ, Dubin AE, Patapoutian A. TRPV3 regulates nitric oxide synthase-independent nitric oxide synthesis in the skin. Nat Commun. 2011; 2:369.doi: 10.1038/ncomms1371 [PubMed: 21712817]
13. Bautista DM, et al. The menthol receptor TRPM8 is the principal detector of environmental cold. Nature. 2007; 448:204–208. [PubMed: 17538622]
14. Nagy I, Rang H. Noxious heat activates all capsaicin-sensitive and also a sub-population of capsaicin-insensitive dorsal root ganglion neurons. Neuroscience. 1999; 88:995–997. [PubMed: 10336113]
15. Woodbury CJ, et al. Nociceptors lacking TRPV1 and TRPV2 have normal heat responses. J Neurosci. 2004; 24:6410–6415. [PubMed: 15254097]
16. Lawson JJ, McIlwrath SL, Woodbury CJ, Davis BM, Koerber HR. TRPV1 unlike TRPV2 is restricted to a subset of mechanically insensitive cutaneous nociceptors responding to heat. J Pain. 2008; 9:298–308. [PubMed: 18226966]
17. Hu HZ, et al. 2-Aminoethoxydiphenyl Borate Is a Common Activator of TRPV1, TRPV2, and TRPV3. J Biol Chem. 2004; 279:35741–35748. [PubMed: 15194687]
18. Birren SJ, Anderson DJ. A v-myc-immortalized sympathoadrenal progenitor cell line in which neuronal differentiation is initiated by FGF but not NGF. Neuron. 1990; 4:189–201. [PubMed: 2155007]
19. Wu L-J, Sweet T-B, Clapham DE. International Union of Basic and Clinical Pharmacology. LXXVI. Current Progress in the Mammalian TRP Ion Channel Family. Pharmacological Reviews. 2010; 62:381–404. Abbreviations. DOI: 10.1124/pr.110.002725 [PubMed: 20716668]
20. Caterina MJ, Rosen TA, Tominaga M, Brake AJ, Julius D. A capsaicin-receptor homologue with a high threshold for noxious heat. Nature. 1999; 398:436–441. [PubMed: 10201375]
21. Vennekens R, Nilius B. Insights into TRPM4 function, regulation and physiological role. Handb Exp Pharmacol. 2007:269–285. [PubMed: 17217063]
22. Togashi K, et al. TRPM2 activation by cyclic ADP-ribose at body temperature is involved in insulin secretion. EMBO J. 2006; 25:1804–1815. [PubMed: 16601673]
23. Naziroglu M, Ozgul C, Celik O, Cig B, Sozbir E. Aminoethoxydiphenyl borate and flufenamic acid inhibit Ca2+ influx through TRPM2 channels in rat dorsal root ganglion neurons activated by ADP-ribose and rotenone. J Membr Biol. 2011; 241:69–75. DOI: 10.1007/s00232-011-9363-9 [PubMed: 21509529]
24. Usoskin D, et al. Unbiased classification of sensory neuron types by large-scale single-cell RNA sequencing. Nature neuroscience. 2014; doi: 10.1038/nn.3881
25. Hara Y, et al. LTRPC2 Ca2+-permeable channel activated by changes in redox status confers susceptibility to cell death. Mol Cell. 2002; 9:163–173. [PubMed: 11804595]
26. Togashi K, Inada H, Tominaga M. Inhibition of the transient receptor potential cation channel TRPM2 by 2-aminoethoxydiphenyl borate (2-APB). Br J Pharmacol. 2008; 153:1324–1330. 0707675 [pii]. DOI: 10.1038/sj.bjp.0707675 [PubMed: 18204483]

27. Yamamoto S, et al. TRPM2-mediated Ca2+influx induces chemokine production in monocytes that aggravates inflammatory neutrophil infiltration. Nat Med. 2008; 14:738–747. nm1758 [pii]. DOI: 10.1038/nm1758 [PubMed: 18542050]

28. Uchida K, et al. Lack of TRPM2 impaired insulin secretion and glucose metabolisms in mice. Diabetes. 2011; 60:119–126. doi:db10-0276 [pii]. DOI: 10.2337/db10-0276 [PubMed: 20921208]

29. Ariza-McNaughton L, Krumlauf R. Non-radioactive in situ hybridization: simplified procedures for use in whole-mounts of mouse and chick embryos. Int Rev Neurobiol. 2002; 47:239–250. [PubMed: 12198801]

30. Schmid D, Messlinger K, Belmonte C, Fischer MJ. Altered thermal sensitivity in neurons injured by infraorbital nerve lesion. Neurosci Lett. 2011; 488:168–172. [PubMed: 21078368]

31. Jang Y, et al. TRPM2 mediates the lysophosphatidic acid-induced neurite retraction in the developing brain. Pflugers Arch. 2014; 466:1987–1998. DOI: 10.1007/s00424-013-1436-4 [PubMed: 24413888]

Europe PMC Funders Author Manuscripts

Europe PMC Funders Author Manuscripts

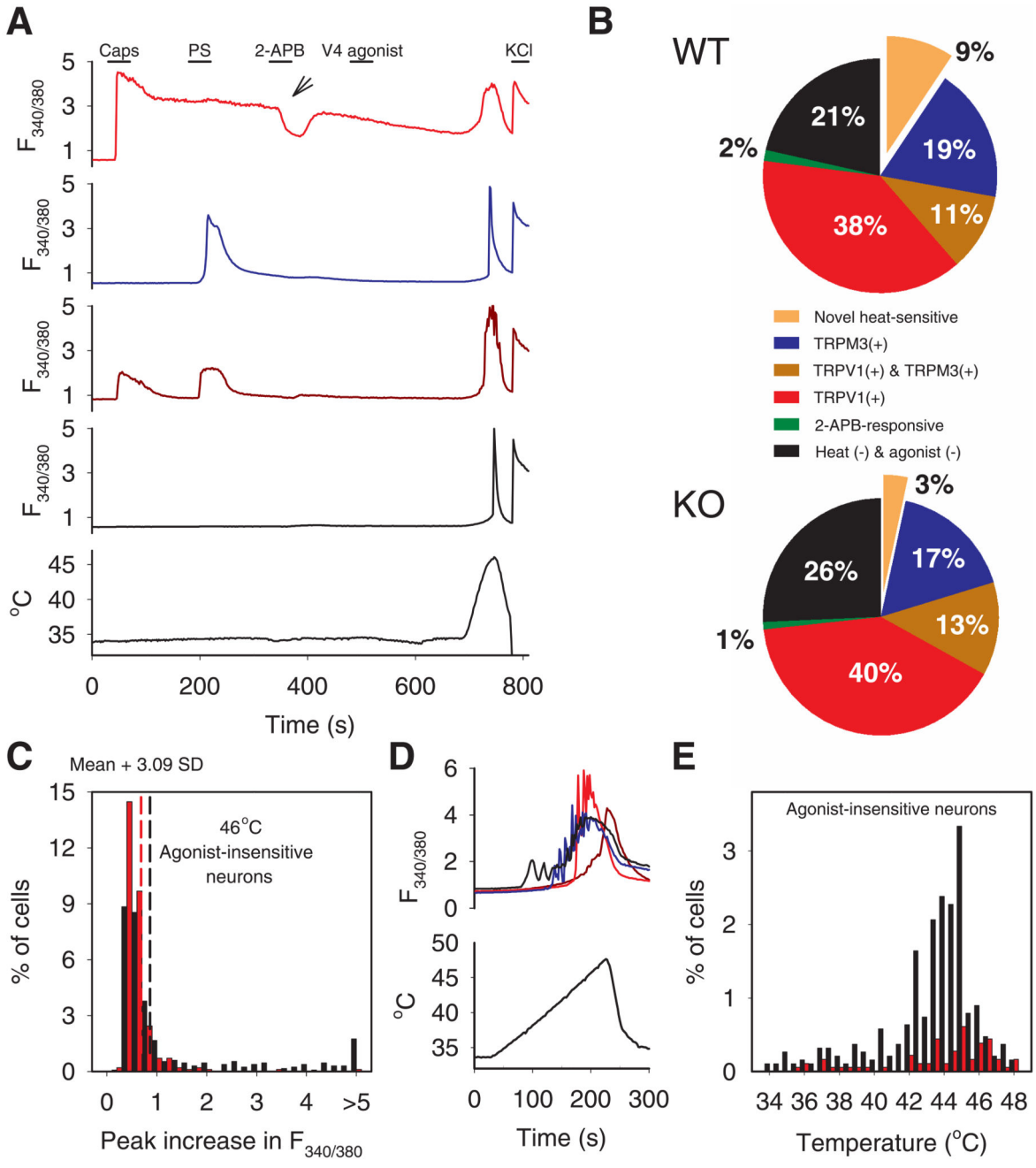

Fig. 1. Around 10% of somatosensory neurons show a novel heat-sensitive mechanism.

A. Examples of increases of $[Ca^{2+}]_i$ measured with fura-2 ($F_{340/380}$ ratio, ordinate) in response to known TRP channel agonists and to heat. From top: TRPV1-expressing neuron responding to capsaicin (caps, red); TRPM3-expressing neuron responding to pregenolone sulphate (PS, blue); TRPV1- and TRPM3- co-expressing neuron (brown); neuron unresponsive to TRP channel agonists but showing a response to heat. See Supplementary Information video 1 for images.

B. Percentages of neurons expressing TRPV1, TRPM3 and the novel heat-sensitive mechanism in DRG neurons from WT (top) and TRPM2$^{-/-}$ mice (bottom). Green: neurons responding to 2-APB but not to other agonists.

C. Histogram of maximal $F_{340/380}$ ratio increase in neurons insensitive to TRP agonists. Black: WT neurons; red: TRPM2$^{-/-}$ neurons. Vertical dashed lines: thresholds discriminating between heat-sensitive and insensitive neurons (see Extended Data Fig. 1 for details).

D. Thermal thresholds of novel heat-sensitive DRG neurons. Increases of $F_{340/380}$ ratio (top) in response to slowly rising heat ramp (bottom).

E. Temperature thresholds of novel heat-sensitive neurons from WT (black) and TRPM2$^{-/-}$ mice (red). Proportion in range 34-42°C reduced from 4.4% in WT to 0.9% in TRPM2$^{-/-}$ ($p \leqq 0.0001$; Fisher's exact test), and in range 42-48°C from 15% in WT (290/1890) to 3% in TRPM2$^{-/-}$ (55/1800) ($p \leqq 0.0001$; Fisher's exact test).

Cell numbers and replicates. A - C: 1324 DRG neurons from one WT mouse on 4 coverslips and 981 DRG neurons from one TRPM2$^{-/-}$ mouse on 4 coverslips were imaged. Similar results obtained using 52 further coverslips from 9 further WT mice and 10 coverslips from 3 further TRPM2$^{-/-}$ mice; some of these results are shown in Extended Data Figs 1, 2 and 4. D, E: 1890 DRG neurons from one WT mouse on 8 coverslips and 1800 DRG neurons from one TRPM2$^{-/-}$ mouse on 8 coverslips were imaged. Similar results obtained using 10 coverslips from 1 further WT mouse.

Europe PMC Funders Author Manuscripts

Europe PMC Funders Author Manuscripts

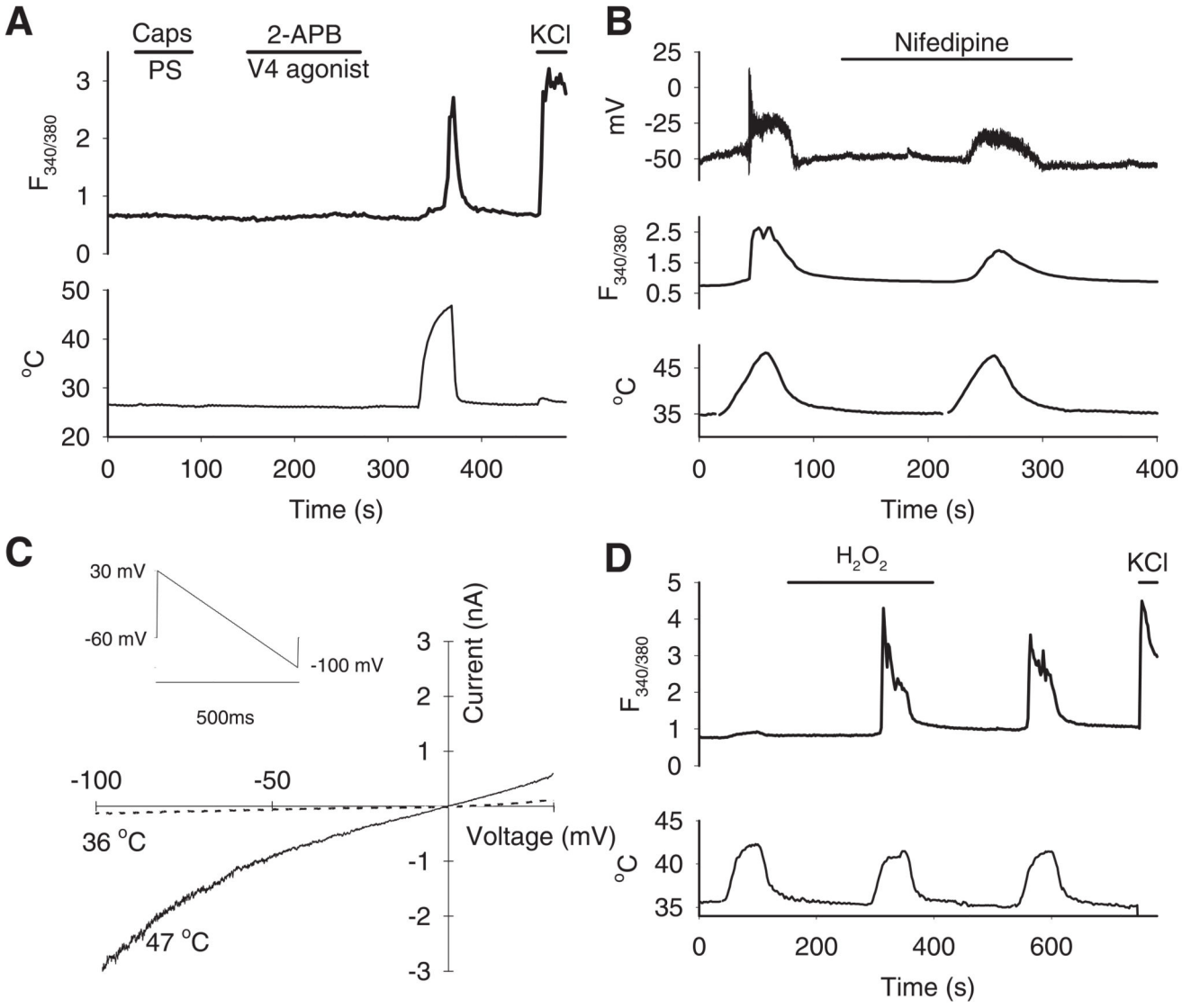

Fig. 2. Properties of the novel heat-sensitive ion channel in autonomic neurons.

A. Sympathetic neurons from superior cervical ganglion (SCG) respond to heat but not to TRP channel agonists.

B. The L-type Ca^{2+} channel blocker nifedipine (10 μM) blocks spiking but not steady depolarization in response to heat in a patch-clamped PPG neuron (top) and reduces but does not eliminate the Ca^{2+} increase (middle). Simultaneous recording of membrane potential and $[Ca^{2+}]_i$ ($F_{340/380}$ ratio) in current–clamped PPG neuron.

C. Current-voltage relations at 36°C and 47°C of voltage-clamped PPG neuron in response to voltage ramp shown top left. Similar IV relation observed with inverse voltage ramp starting from 100mV (Extended Data Fig. 7). See Methods for details.

D. H_2O_2 (400μM) potentiates Ca^{2+} increase in response to a mild temperature stimulus (42°C) in SCG neurons. Note potentiation is long-lasting after H_2O_2 removed. Similar results obtained in PPG neurons. Percentage of neurons (n=456) responding to heat, determined as in Extended Data Fig. 1B, was 5% before, 59% during and 54% post-H_2O_2.

Cell numbers and replicates. A: 166 SCG neurons from 3 WT mice on 3 coverslips were imaged for this experiment. Similar results obtained with SCG neurons using 15 further coverslips from 9 further mice and with PPG neurons using 14 coverslips from 9 further mice. B: 2 PPG neurons on 2 coverslips were simultaneously patch-clamped and imaged and showed a similar response. C: 3 PPG neurons on 3 coverslips were simultaneously patch-clamped and imaged and showed a similar response. D: 456 SCG neurons from two WT mice on 4 coverslips were imaged and showed a similar enhancement with H_2O_2; 731 PPG neurons (not shown) from three WT mice on 3 coverslips were imaged and showed a similar enhancement to the SCG neurons. Similar results obtained with SCG neurons using 9 coverslips from 5 further mice and with PPG neurons using 3 coverslips from 3 further mice.

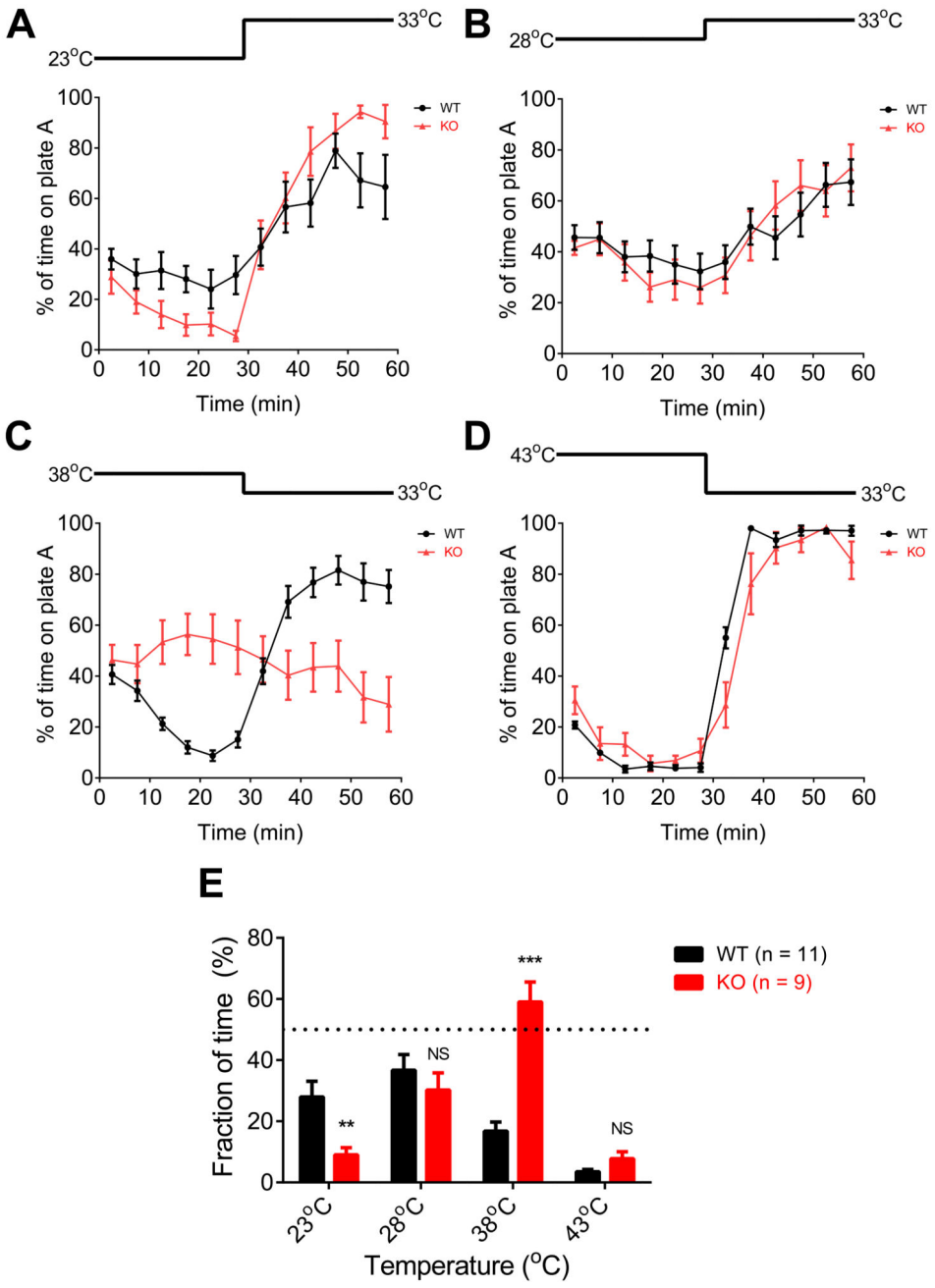

Figure 3. Deletion of TRPM2 shifts adult male mouse thermal preference towards warmer temperatures.

A-D: Two-plate thermal preference test. One plate is at 33°C at the start of the experiment, the other ("plate A") is at a variable temperature as shown above each graph. Temperature reversed at t= 30min to account for any possible bias caused by external cues. Points show mean behavioural preference averaged over 5 min intervals (error bars mean ± SEM, n = 11 for WT and 9 for TRPM2$^{-/-}$). Mice were WT or TRPM2$^{-/-}$ male littermates, 12-16 weeks of age. No difference observed between the thermal behaviour of WT and heterozygous TRPM2$^{+/-}$ mice (not shown, n = 4).

E: Mean thermal preference averaged from the data between t = 15-30min and t = 45-60 min shown in A-D. Bars give mean ± SEM. **, $p < 0.01$; ***, $p < 0.001$; NS, $p > 0.05$; unpaired t-test.

Biological replicates. Similar results were obtained with experiments using non-littermates in which 12 WT male mice from Charles River were compared with 7 TRPM2$^{-/-}$ male mice from homozygote breeding pairs.

Europe PMC Funders Author Manuscripts

Table 1

mRNA levels of TRP ion channel genes in MAH cells in growth medium containing dexamethasone (5 μM) and in differentiation medium containing growth factors bFGF (10 ng/ml), CNTF (10 ng/ml) and NGF (50 ng/ml).

All genes within the TRP channel family and the six cyclic nucleotide-regulated channels (CNGA1-4, CNGB1, and CNGB3) were examined. The seven genes listed are the ones whose mRNA levels are detectable in MAH cells in either condition. FPKM is fragments per kilobase of transcript per million mapped reads. The p values give significance of change of expression using one-way Anova; q-values are post-hoc corrected for multiple testing using the False Discovery Rate (FDR) method. Two biological replicates in each condition were deep-sequenced.

Gene	FPKM in growth medium	FPKM in differentiation medium	Log_2 fold change	p value	q value
TRPC1	1.779	4.700	1.401	<0.001	<0.001
TRPC2	6.804	4.995	-0.446	0.121	0.323
TRPC3	5.641	1.309	-5.729	<0.001	<0.001
TRPV2	0.035	4.003	6.840	<0.001	<0.001
TRPM2	1.017	0.970	-0.069	0.800	0.922
TRPM4	0.277	0.400	0.532	0.112	0.310
TRPM7	18.108	15.428	-0.231	0.196	0.428